AGU ADVANCING EARTH AND SPACE SCIENCES

Water Resources Research

RESEARCH ARTICLE
10.1029/2023WR036139

Land Surface Modeling as a Tool to Explore Sustainable Irrigation Practices in Mediterranean Fruit Orchards

O. Dombrowski[1], C. Brogi[1], H.-J. Hendricks Franssen[1], V. Pisinaras[2], A. Panagopoulos[2], S. Swenson[3], and H. Bogena[1]

[1]Agrosphere (IBG-3), Forschungszentrum Jülich GmbH, Jülich, Germany, [2]Soil & Water Resources Institute, Hellenic Agricultural Organization, Thessaloniki, Greece, [3]Climate and Global Dynamics Laboratory, National Center for Atmospheric Research, Boulder, CO, USA

Key Points:

- The CLM5 irrigation routine is tested at different scales and enhanced with the option to prescribe irrigation amounts and schedules
- Soil moisture dynamics were simulated well but model simplifications limit the ability of CLM5 for field-scale irrigation scheduling
- Regional simulations using different irrigation scenarios identified priorities and water savings for improved irrigation management

Correspondence to:
O. Dombrowski,
o.dombrowski@fz-juelich.de

Citation:
Dombrowski, O., Brogi, C., Hendricks Franssen, H.-J., Pisinaras, V., Panagopoulos, A., Swenson, S., & Bogena, H. (2024). Land surface modeling as a tool to explore sustainable irrigation practices in Mediterranean fruit orchards. *Water Resources Research*, *60*, e2023WR036139. https://doi.org/10.1029/2023WR036139

Received 14 SEP 2023
Accepted 24 JUN 2024

Author Contributions:
Conceptualization: O. Dombrowski, C. Brogi, H.-J. Hendricks Franssen, H. Bogena
Data curation: O. Dombrowski
Formal analysis: O. Dombrowski, C. Brogi
Funding acquisition: V. Pisinaras, A. Panagopoulos, H. Bogena
Investigation: O. Dombrowski, C. Brogi, V. Pisinaras, A. Panagopoulos
Methodology: O. Dombrowski, C. Brogi, H.-J. Hendricks Franssen, H. Bogena
Project administration: V. Pisinaras, A. Panagopoulos, H. Bogena
Resources: H.-J. Hendricks Franssen, V. Pisinaras, A. Panagopoulos, H. Bogena
Software: O. Dombrowski, S. Swenson

Abstract Irrigation strongly influences land-atmosphere processes from regional to global scale. Therefore, an accurate representation of irrigation is crucial to understand these interactions and address water resources issues. While irrigation schemes are increasingly integrated into land surface models, their evaluation and further development remains challenging due to data limitations. This study assessed the representation of field-scale irrigation using the Community Land Model version 5 (CLM5) through comparison of observed and simulated soil moisture, transpiration and crop yield. Irrigation was simulated by (a) adjusting the current irrigation routine and (b) by implementing a novel irrigation data stream that allows to directly use observed irrigation amounts and schedules. In a following step, the effect of different irrigation scenarios at the regional scale was simulated by using this novel data stream. At the plot scale, the novel irrigation data stream performed better in representing observed SM dynamics compared to the current irrigation routine. Nonetheless, simplifications in crop and irrigation representation and uncertainty in the relation between water stress and yield currently limit the ability of CLM5 for field-scale irrigation scheduling. Still, the simulations revealed valuable insights into model performance that can inform and improve the modeling beyond the field scale. At regional scale, the simulations identified irrigation priorities and potential water savings. Furthermore, application of LSMs such as CLM5 can help to study the effects of irrigation beyond water availability, for example, on energy fluxes and climate, thus providing a powerful tool to assess the broader implications of irrigation at larger scale.

Plain Language Summary Irrigation impacts how land and atmosphere interact, both locally and globally. Therefore, it is important to understand the effects of irrigation practices and improve how water resources are managed. Advanced models such as land surface models now include irrigation. However, developing these models is difficult due to limited data. This study used the Community Land Model version 5 (CLM5) to compare observed and simulated soil moisture, plant water use, and crop yield. Two methods were used: an updated irrigation routine and a new data stream that uses actual irrigation amounts and schedules. The new data stream more accurately represented soil moisture. Simplifications in how the model handles crops and irrigation, and uncertainty about the link between water stress and yield, limit CLM5's effectiveness for precise irrigation planning. Still, the simulations provided valuable insights into the model's performance. At a regional level, the simulations highlighted key areas for irrigation and potential water savings. Models like CLM5 can help study the effects of irrigation on water availability, energy fluxes, and climate, making them useful tools for improving water management and allocation.

1. Introduction

Irrigation plays a vital role in sustaining global food production by providing a reliable water supply to agricultural systems, especially in semi-arid or arid regions (McLaughlin & Kinzelbach, 2015). Irrigation contributes significantly to food security by enabling higher crop yields and reducing the vulnerability of agricultural systems to climate change, which is key in light of the growing population and increasing food demands (McDermid et al., 2023; Mueller et al., 2012). On the other hand, poor management of irrigation water has led to the depletion of groundwater resources (Dangar et al., 2021; Scanlon et al., 2012; Wada et al., 2010) and water use conflicts in many regions (Cai et al., 2003; Eshete et al., 2020; Gurung et al., 2006). Apart from quantitative and qualitative effects on water resources (García-Garizábal et al., 2012; Y Zhang et al., 2022), irrigation substantially impacts biogeophysical and biogeochemical processes at the land surface through alteration of the hydrological cycle or

Supervision: C. Brogi, H.-J. Hendricks Franssen, H. Bogena
Visualization: O. Dombrowski
Writing – original draft: O. Dombrowski
Writing – review & editing: O. Dombrowski, C. Brogi, H.-J. Hendricks Franssen, V. Pisinaras, A. Panagopoulos, S. Swenson, H. Bogena

energy budget with direct effects on climate (DeAngelis et al., 2010; Erb et al., 2017; Ferguson & Maxwell, 2012; Gordon et al., 2005; Sacks et al., 2009). The multidimensional role of irrigation calls for increased efforts in effective irrigation management and irrigation impact studies using large-scale and comprehensive approaches. This is crucial not only to meet food demands and mitigate future increases in climate change induced water stress, but also to understand its interactions and feedback mechanisms within the Earth system (Elliott et al., 2014; McDermid et al., 2023).

Modeling can be a powerful tool to simulate complex interactions in agricultural systems, evaluate different irrigation and climate scenarios, and provide decision support for water resources management (Blyth et al., 2021; Pongratz et al., 2018). This necessitates comprehensive modeling frameworks that combine field-scale representations of crop growth and irrigation with a more holistic assessment of the impacts of irrigated agriculture on water resources and climate at larger scale (Bin Peng et al., 2020). Process-based crop models include a range of crop parameterizations that provide a unique way to study crop growth processes in response to irrigation practices by using physical and biological principles. However, their main purpose is to simulate yield at the field scale, often over a single growing season, while lacking the interface with the land surface, soil, and climate (Cheng et al., 2020). Land surface models (LSMs), on the other hand, provide a more holistic representation of the land-atmosphere interactions to capture the feedback mechanisms between irrigation, vegetation, hydrological processes, and climatic conditions beyond the field scale (Blyth et al., 2021). Conversely, they often lack more detailed physiological and genetic representations of crops and irrigation management (Lombardozzi et al., 2020; B Peng et al., 2018). This limits the ability of LSMs to reliably simulate yield and irrigation water withdrawals leading to poor model performance and biases in related processes such as carbon, energy, and water fluxes over intensively irrigated regions (Leng et al., 2015; Lombardozzi et al., 2020; Ozdogan et al., 2010; *Z* Zhang et al., 2020).

In recognition of the important role of human land management, efforts to advance the representation of crops and irrigation in LSMs are ongoing (Pokhrel et al., 2016). Various land surface models such as ORCHIDEE, the Community Land Model (CLM), and Noah-MP have since added crop modules (Levis et al., 2012; Liu et al., 2016; Smith et al., 2010). New crop representations have been developed to improve crop growth and management processes (Boas et al., 2021; B Peng et al., 2018) or to add new crop types (Dombrowski et al., 2022; Fader et al., 2015; Fan et al., 2015). Rather simple irrigation schemes are generally incorporated based on soil moisture thresholds (de Vrese et al., 2016; Ozdogan et al., 2010; Sacks et al., 2009), while more recent developments include the integration of irrigation techniques (Leng et al., 2017; Yao et al., 2022), irrigation water withdrawal from different sources (Leng et al., 2017; Xia et al., 2022), and water availability limitation (Yin et al., 2020) into various LSMs. These studies, however, were performed at river basin, county, or global level with coarse spatial resolutions between 10 and 100 km using global or national maps of the irrigated area to define the spatial distribution of irrigation (Leng et al., 2014; Ozdogan & Gutman, 2008; Siebert et al., 2005). Also, simulated irrigation was calibrated or validated against rather uncertain statistics like total yearly irrigation water withdrawals at the county level or coarser. More recently, Lawston et al. (2017) evaluated the irrigation scheme of the NASA Land Information System LSM with point and gridded SM observations at 1 km resolution. While the model could represent the seasonal variability and regional average SM dynamics, it did not capture the field-scale heterogeneity and overestimated irrigation amounts. Another recent study used the dynamic crop and irrigation scheme of the Noah-MP LSM to examine the effect of different irrigation setups on maize yield in order to recommend an optimal SM threshold to trigger irrigation (Huang et al., 2022).

However, these studies had a rather coarse resolution and either did not consider specific irrigation practices such as irrigation timing, or lacked data to accurately assess the simulated irrigation amount and crop yield. Additional field-scale crop and irrigation data is needed to evaluate the performance of irrigation schemes currently implemented in LSMs. Assessments at high spatial resolution such as the field scale are especially important so that the implications of irrigation practices for regional water resources management can be reliably investigated. The work presented here addresses this need by performing a comprehensive field-scale validation of the irrigation routine of the latest version of CLM (CLM5). Specifically, we evaluate the flexibility of the existing irrigation routine of CLM5 to represent locally observed irrigation schedules. We then implement a new model capability to use the observed irrigation schedule as model input and compare the resulting simulations to observed SM, transpiration, and yield at the field scale. Subsequently, we perform catchment-scale CLM5 simulations with a high resolution of 1 ha to examine the effect of different irrigation scenarios at the catchment scale and discuss the implications for irrigation and water resources management.

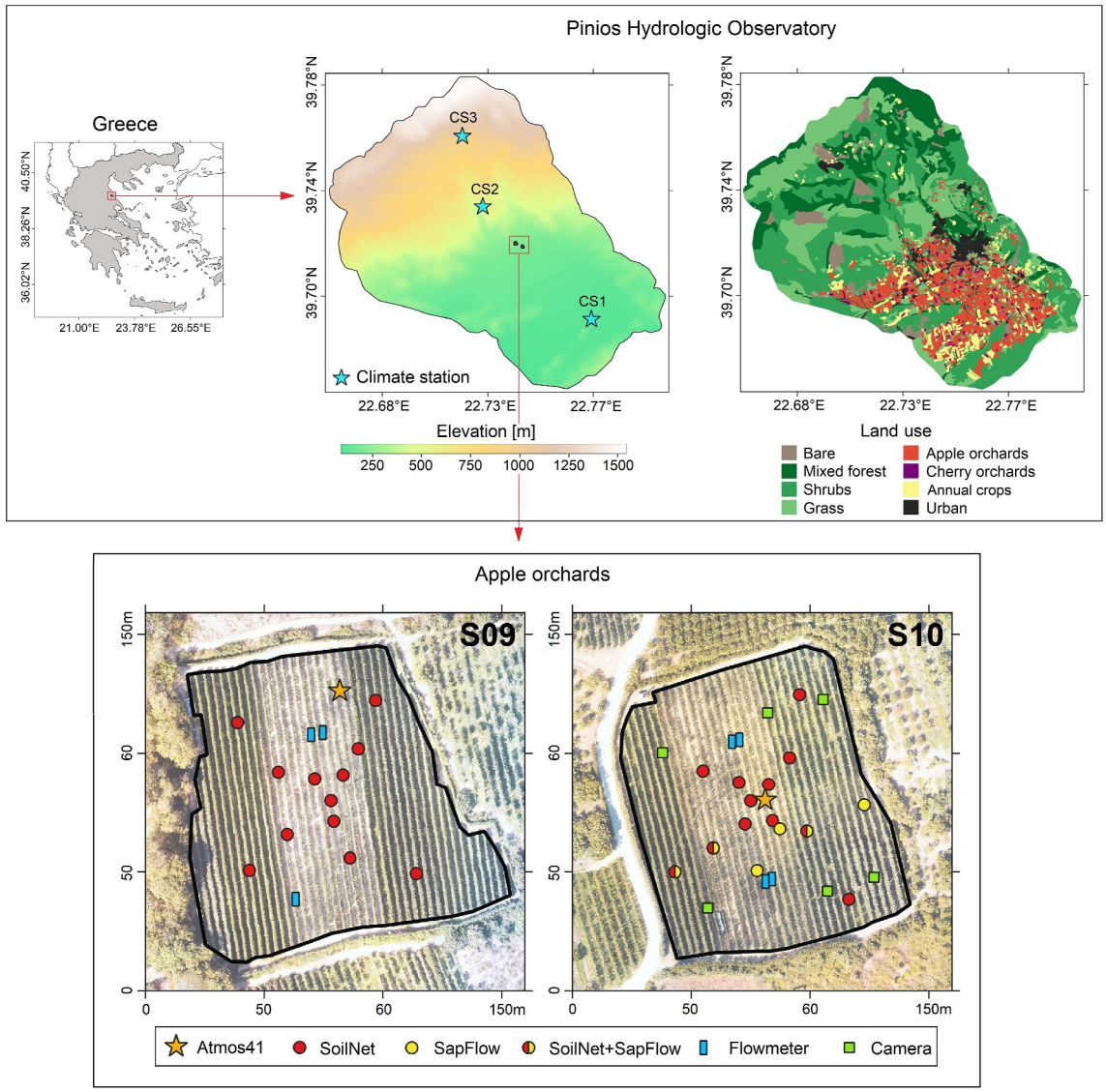

Figure 1. Top left: Map overview of Greece and of the study area location. Top right: Elevation and land use of Pinios Hydrologic Observatory with the locations of climate stations. Bottom: Apple orchards S09 and S10 with instrumentation.

2. Materials and Methods

2.1. Study Area

Located in central Greece, the Pinios Hydrologic Observatory (PHO) covers an area of approximately 45 km^2 (Figure 1). The PHO was established in 2015 to study the Pinios catchment hydrological processes and, ultimately, to support local authorities in the sustainable management of water resources (V Pisinaras et al., 2018). It is characterized by a Mediterranean climate with an annual precipitation of 500–1,200 mm, and highest precipitation amounts in the winter months, annual potential evapotranspiration of approximately 1,100 mm, and annual average air temperature of 15°C (Bogena et al., 2018). The area displays a range of altitudes from 1,500 m in the northern part down to less than 200 m in the plain. The mountainous part of the catchment features steep slopes and is covered by forests, mixed with shrubs and grassland, while the southern plain is primarily characterized by agriculture and small villages. In the plain, sandy loam soils dominate while sandy clay loam and loamy soils also occur (V Pisinaras et al., 2018). The PHO is located in one of the most productive agricultural areas in Greece owing, among other factors, to widespread irrigation practices that account for over 85% of the local freshwater consumption (Panagopoulos et al., 2018). The main cultivation are apple and cherry orchards

Table 1
Main Characteristics of the Two Apple Orchards (S09 and S10)

Orchard ID	Altitude (m.a.s.l.)	Size (ha)	Apple varieties	Soil depth (cm)	Sand content (%)	Clay content (%)	Soil organic carbon content (%)	Gravel content (%)
S09	200	1.24	3	0–30	64.5	17.8	1.5	23.3
				30–60	63.0	21.9	1.2	20.6
				60–90	59.9	24.6	0.7	13.7
S10	190	1.13	5	0–30	64.3	12.5	1.44	28.2
				30–60	65.8	12.7	0.86	28.7
				60–90	65.4	13.7	0.66	28.7

(i.e., ~78% of agricultural area) that are irrigated between May and October. There are a few other rainfed fruit and nut tree orchards in the area with <5% coverage. Annual crops including corn, cereal (mainly winter wheat), and potato are grown on the remaining agricultural land. They are partially irrigated, depending on precipitation occurrence, but cover a negligible part of the total irrigated area. Irrigation in the orchards is typically applied through micro sprinklers and the demand is almost entirely met by abstraction from the alluvial groundwater system through water wells, most of which are privately owned. Overexploitation of groundwater in the area due to poor irrigation management practices, amongst others, has previously been reported by Panagopoulos et al. (2018) and Vassilios Pisinaras et al. (2023) resulting in the decline of groundwater levels.

Within the PHO, irrigation management in two irrigated apple orchards, hereafter referred to as S09 and S10, was studied (Figure 1). Both orchards have a size of around 1.2 ha, with a mild southern slope of <5%. The soil texture is sandy loam and sandy clay loam with a high gravel content (13%–29%) (Table 1) and many larger cobbles (>64 mm according to Wentworth (1922)), especially below 30–50 cm depth. Trees are planted in rows, oriented North-South with 3.3 m distance between rows and an in-line distance of 1.5 m (approximately 2,020 trees ha^{-1}). The trees in S09 and S10 were planted in 2013 and 2015 respectively, with a mixture of 3–5 different varieties. Trees are pruned to a height of 3.5 m throughout the winter season and residues are mulched back into the soil. Bud burst typically occurs in the second half of March while fruit development starts with the end of flowering in mid to late April. Harvest dates range from late August to mid-November depending on the harvested variety. Major leaf fall starts in late October and continues until mid-November, sometimes until early December. Trees are irrigated with a micro sprinkler system with a maximum flow rate of 60 L hr^{-1} that is installed below the canopy, halfway between the tree stems of the same row. The irrigation season typically starts in May and continues until October. Orchards are fertilized with 80 kgN ha^{-1} at the end of flowering in April. Pest and fungicide treatment is applied prior to flowering and after flowering until late June. The grass in the alleys is generally mowed once a month starting in March or April and mowing material is left on the ground. During periods of intense heat, the actively growing grass cover provides a cooling effect to protect the apples from heat damage.

3. Data Sources

The meteorological data that are necessary to drive CLM5 including precipitation, air temperature, atmospheric pressure, wind speed, relative humidity, and incoming solar radiation, were acquired from three meteorological stations located at different altitudes within the PHO (Figure 1) as well as two stations located in the orchards S09 and S10. For the agricultural plain, detailed soil texture and organic matter information was collected during an extensive soil sampling campaign. In total, 116 locations were sampled with one sample from the topsoil (0–50 cm) and a second sample from the subsoil (50–100 cm) (Figure 2). In addition to the point measurements, the LUCAS topsoil physical properties for Europe soil map (Ballabio et al., 2016) and the European Soil Database (ESDB) derived data product (Hiederer, 2013) provide soil information for the area at a resolution of 500 × 500 and 1,000 × 1,000 m, respectively (Table 2). These data sources were combined to create soil texture (point measurements + LUCAS) and soil organic carbon (point measurements + ESDB) maps for model input (Figure 2). In a first step, for the unsampled regions, data points were extracted from the map products in a sampling density equal to the average density of the soil sampling locations (~580 × 580 m). Next, the extracted points were combined with the sampled points to a single set of data points (Figure 2). Then, the points were interpolated to the target resolution of 100 × 100 m using ordinary kriging and a spherical variogram model with a

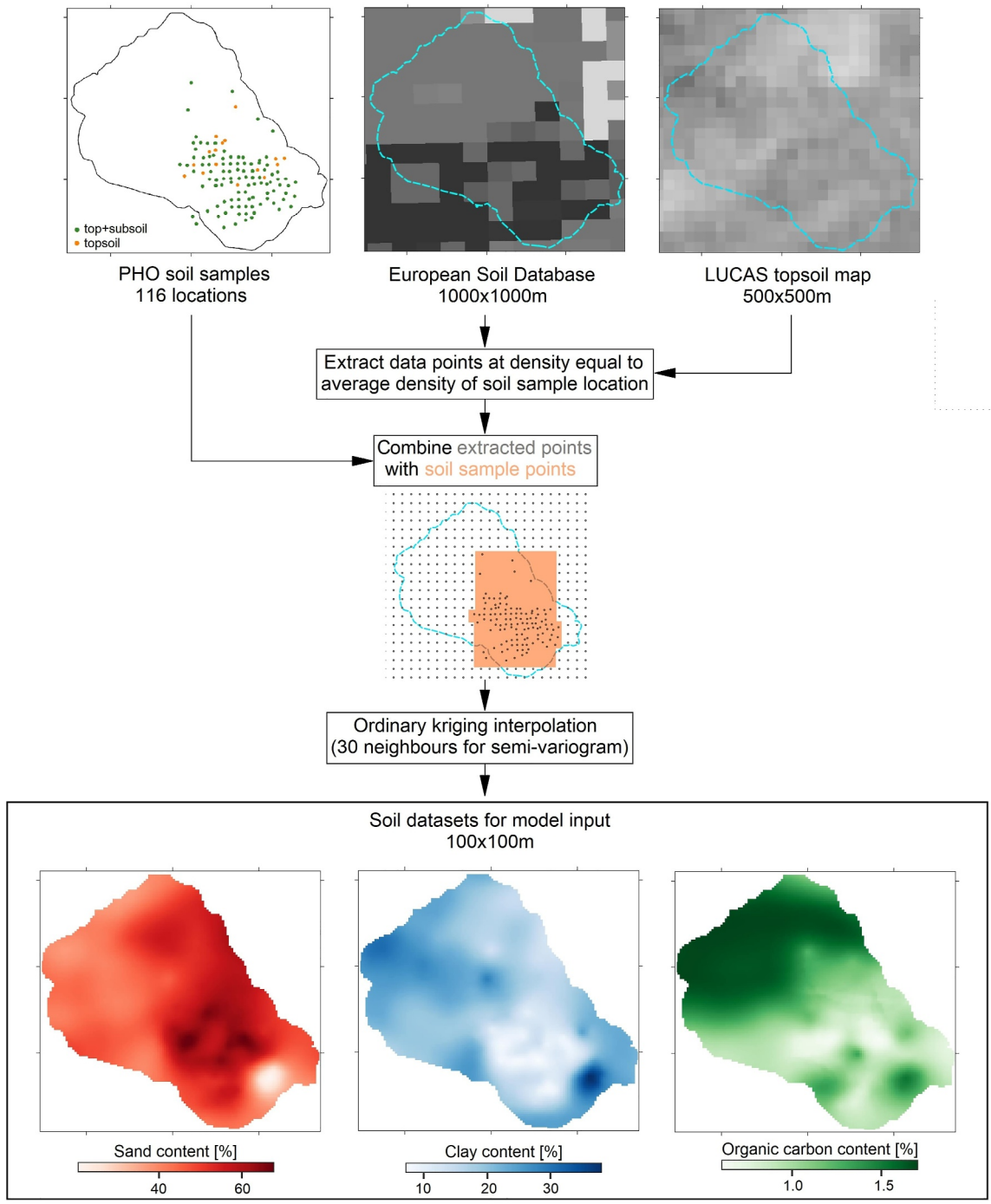

Figure 2. Top, from left to right: Soil sampling locations within the Pinios Hydrologic Observatory, soil data from the European soil database and the LUCAS topsoil map. Bottom: Soil texture input datasets of sand, clay, and organic carbon derived from the three data sources.

radius that included 30 measurements around an estimation point. Topographic information was available through the European Digital Elevation Model (EU-DEM) (Copernicus, 2016), version 1.1 at a spatial resolution of 25 × 25 m (Figure 1). Detailed maps of the agricultural fields and orchards were provided by the Hellenic Payment and Control Agency for Guidance and Guarantee Community Aid while the land use of the remaining area was digitized from satellite imagery, using ArcGIS® software by Esri (Figure 1).

Table 2
Main Characteristics of the Different Soil Data Products Used for the Surface File Creation of the Regional Case

	European soil database derived data	LUCAS topsoil physical properties for europe
Underlying observational data	European Soil Database, Harmonized World Soil Database, Soil-Terrain Database	LUCAS 2009 soil survey (around 20,000 points) for EU-25
Resolution (m)	1,000 × 1,000	500 × 500
Soil texture	Yes	Yes
Organic matter	Yes	No
Depth ranges (cm)	0-30, 30-100	0–20

Orchard scale SM data were retrieved from S09 to S10, which were equipped for extensive monitoring in September 2020 (Figure 1). SM was monitored via a SoilNet wireless sensor network (Bogena et al., 2010; Bogena et al., 2022) with 12 nodes per orchard. Each node had six SMT100 SM sensors (Truebner GmbH, Neustadt, Germany) divided into two separate profiles which were installed at 5, 20, and 50 cm depth as well as two TEROS21 soil matric potential (SMP) sensors (METER Group Inc., Pullman, USA) installed at 20 cm depth. Irrigation amounts were recorded at 15 min intervals with TW-N flowmeters (TECNIDRO, Genova, Italy) connected to LR35 data loggers (Delta OHM, Italy). The flowmeters were installed downstream of the valves of each irrigation sector within the orchards (three sectors in S09 and four sectors in S10). Irrigation sectors were irrigated at the same time but received different water volumes depending on their size. To obtain a single irrigation time series per orchard, measured hourly irrigation volumes in each irrigation sector were summed up and converted to mm using their combined irrigated area. Meteorological data was collected by the cost-effective but reliable all-in-one Atmos41 weather station (METER Group Inc., Pullman, USA) installed above the canopy in each orchard (Dombrowski et al., 2021). A more detailed description of the instrumentation and setup used to monitor SM dynamics, irrigation, and meteorological variables is given in Brogi et al., 2023. Additionally, S10 was equipped with six SFM-1 sapflow sensors (ICT International Pty Ltd, Armidale, Australia) to estimate whole-tree transpiration. The sapflow sensors were installed on the trunk of six trees to represent, as much as possible, the orchards' trees in terms of height, perimeter, and vigor covering all five varieties. The installation and data correction followed the procedure outlined in Burgess, 2018. Phenology of the three main apple varieties was monitored using six phenocams (SnapShot Cloud 4G, Dörr GmbH, Germany) installed in S10.

3.1. The Land Surface Model

3.1.1. The Community Land Model

The Community Land Model v.5 (CLM5) used in this study is the latest version of the land component in the Community Earth System Model (CESM) as described in detail by D M Lawrence et al. (2019). CLM5 simulates land surface energy fluxes as well as hydrological, biogeophysical, and biogeochemical processes that are driven by atmospheric input variables in combination with soil and vegetation states and characteristics (D Lawrence et al., 2018). These processes are simulated on different subgrid units within a grid cell. Subgrid units include (a) the land unit defining the land use category (e.g., vegetated, urban, crop), (b) the column that is represented by 20 soil and 5 bedrock layers and resolves state variables and fluxes of water and energy in the soil, and (c) the patch level capturing biogeophysical and biogeochemical differences between plant functional types (PFTs) (e.g., broadleaf deciduous forest, evergreen shrub, maize, soy). The one-dimensional multilayer vertical water flow in the soil is simulated using a modified Richards equation (Dingman, 2015). Soil hydraulic parameters for these calculations are derived from pedotransfer functions of sand and clay (Clapp & Hornberger, 1978; Cosby et al., 1984) and organic properties of the soil (D Lawrence & Slater, 2008). With version five of CLM, a plant hydraulic stress routine was introduced that uses a simple hydraulic framework to model water transport along a water potential gradient from soil via plant to atmosphere (Kennedy et al., 2019). The new configuration replaces soil potential with leaf potential as the basis for plant water stress while root water potential is used to drive root water uptake. A new biogeochemistry and crop module, BGC-Crop, enhanced the representation of major crop functional types and land management practices such as irrigation and fertilization. Unlike natural vegetation that competes for water and nutrients, crops operate on separate soil columns that may be irrigated or non-irrigated, thus allowing for differences in land management (D M Lawrence et al., 2019).

The recent development of CLM5-FruitTree enables the simulation of deciduous fruit trees and associated management practices in CLM5. The main features of the new sub-model include (a) a perennial phenology routine that allows the woody plant parts to remain on the orchard for several years, (b) carbon storage dynamics that enable the regrowth of annual plant parts, (c) an adapted carbon and nitrogen allocation, and (d) the description of typical management practices such as transplanting, pruning, and orchard rotation. Additionally, a new apple plant functional type was parameterized while fertilization and irrigation use the default CLM5 schemes. The complete model development of CLM5-FruitTree is described in Dombrowski et al. (2022).

3.1.2. CLM5 Irrigation Routine

Irrigation is performed individually over each irrigated soil column and responds dynamically to SM based on a daily check at 6 a.m. If crop leaf area is non-zero and if the available soil water over a specified irrigation depth z_{irrig} (=0.6 m by default) is below a defined threshold, irrigation is triggered. The irrigation amount is based on the SM deficit (D_{irrig}) that is calculated over z_{irrig}:

$$D_{irrig} = w_{thresh} - w_{avail} \tag{1}$$

where W_{avail} is the available SM (mm) and W_{thresh} is the irrigation SM threshold (mm) calculated as:

$$w_{thresh} = f_{thresh}(w_{target} - w_{wilt}) + w_{wilt} \tag{2}$$

where w_{target} is the irrigation target SM (mm), w_{wilt} is the SM at wilting point (mm), and f_{thresh} is a tuning parameter. If $f_{thresh} = 1$ (default), irrigation will be triggered once the available SM is below w_{target}. If $f_{thresh} = 0$, irrigation is only triggered once the available SM falls below w_{wilt}. Target SM is determined as the sum of SM at the target SM of each soil layer:

$$w_{target} = \sum_{i=1}^{n_{irr}} \theta_{target,i} * \Delta z_i \tag{3}$$

where n_{irr} is the index of the soil layer corresponding to z_{irrig}, Δz_i (mm) is the depth of the soil layer i and $\theta_{target,i}$ is the target volumetric SM value in a given soil layer. Similarly, w_{wilt} is calculated as the sum of SM at wilting point of each soil layer:

$$w_{wilt} = \sum_{i=1}^{n_{irr}} \theta_{wilt,i} * \Delta z_i \tag{4}$$

where $\theta_{wilt,i}$ is the volumetric SM value at wilting point in a given soil layer. θ_{target} and θ_{wilt} are calculated by inverting the equation for soil matric potential (SMP) (Eq. 7.53 in D Lawrence et al. (2018)) at the respective depth. By default, the SMP parameters ψ_{target} and ψ_{wilt} are set to −34 and −1,500 kPa, considered field capacity and permanent wilting point, respectively.

In addition to w_{target}, w_{wilt}, f_{thresh}, and z_{irrig}, the user can define the irrigation duration (T_{irrig}). Irrigation is applied directly to the ground surface at an intensity equal to $\frac{D_{irrig}}{T_{irrig}}$. Irrigation parameters are not spatially distributed but are defined globally for a given model domain independent of geographic location or crop type.

3.1.3. Irrigation Data Stream Implementation

The above-described irrigation routine uses internal model information to determine the irrigation amount under the absence of observed irrigation amounts. It can be adjusted mainly by the parameters ψ_{target} and f_{thresh} to indirectly approximate these irrigation amounts. However, studying and evaluating the model outcomes under specific observed irrigation schedules and amounts is nearly impossible with the current CLM5 irrigation routine. Therefore, an irrigation data stream was implemented in CLM5 that enables continuous prescription of irrigation parameters, that is, irrigation rate, duration, and start time. These parameters can be defined separately for one or multiple crop types and for each grid cell thus adding new flexibility to the simulations. In this way, differences in

Table 3
Local Crop Parameters for the Apple Plant Functional Type

Parameter	Variable name (unit)	Value
Base temperature for bud burst prediction and GDD summation	baset (°C)	8.5
Chilling requirements for bud burst	crequ (chill days)	−126
Critical temperature to initiate leaf offset	crit_temp (K)	281.15
Final root allocation coefficient until harvest	arootf2 (unitless)	0.12
GDD needed from bud break to canopy maturity	lfmat (°days)	1,350
GDD needed from bud break to harvest	hybgdd (°days)	2100
GDD needed from bud break to the fruit ripening phase	grnrp (°days)	640
GDD needed from bud break to the start of fruit development	grnfill (°days)	130
Initial leaf allocation coefficient	fleafi (unitless)	0.25
Maximum canopy height	ztopmx (m)	3.65
Maximum harvest date in the northern hemisphere	max_NH_harvest_date (mmdd)	1,120
Maximum LAI	laimx (m^2 m^{-2})	2.1
Maximum rooting depth	root_dmx (m)	0.6
Planting density	nstem (# m^{-2})	0.202
Ratio of height: radius at breast height	taper (unitless)	95
The slope of the relationship between leaf N per unit area (gN/m2) and Vcmax25top (umol CO2/m2/s)	s_vcad (μmol CO_2 s^{-1} gN^{-1})	30

irrigation management depending on crop type and location can also be considered which allows to accurately reproduce local management practices or to test any desired irrigation strategy. In addition, the data stream can be used to easily adjust the amount of irrigation applied in order to create different irrigation scenarios (e.g., deficit or over-irrigation) while maintaining the same irrigation schedule. As irrigation is user-defined, the irrigation SM threshold, which is calculated in the CLM5 irrigation routine, is not needed for this implementation.

3.2. Model Set-Up

3.2.1. Orchard Scale Simulations

For the simulations of S09 and S10, CLM5-FruitTree was run in single point mode and forced with hourly meteorological data from the two orchards. Fertilizer amount and soil texture were adjusted according to information provided by the farmer and soil samples. The default parameter file was adapted to account for the local climate and orchards characteristics. Crop parameters such as the different phenological stages were adjusted according to observations from the phenocam pictures, harvest information, and communication with the farmer. In the absence of observed bud break dates, parameters for the bud break prediction model were calibrated such that bud break would occur around the estimated date of fifteenth of March using the available local climate data. The modified crop parameters are listed in Table 3. Additionally, the observed irrigation time series was used as input to the irrigation data stream.

In order to balance ecosystem carbon and nitrogen pools and total water storage in CLM5 (D Lawrence et al., 2018), a 200 yrs model spin-up was performed. For this, the CRUNCEPv7 atmospheric forcing data set from 1986 to 2016 (Viovy, 2018) and the parameterized apple plant functional type were used. Using the model state at the end of the spin-up, simulations were then re-initiated from planting in 2013 (S09) and 2015 (S10) using meteorological data from climate station CS1 (2016–2020) and data from the Atmos41 sensors installed in the orchards for the years 2021 and 2022.

3.2.2. Regional Case Simulations

A regional model domain, encompassing the entire PHO, was set up at a spatial resolution of 1 ha. This resolution was a compromise between accounting for the diverse, patchy landscape with small field and orchard sizes (from a few 100 m^2 to some hectares) and a reasonable computational effort. For the land use information, the database

of agricultural fields and orchards was combined with the remaining land uses digitized from satellite imagery. Since CLM5 allows to define fractional land use in a single grid cell, the overall area of individual land use classes was still accurately represented.

The slope of the terrain was derived from the EU-DEM. Furthermore, the surface parameter defining the depth to bedrock was adjusted based on the minimum (0.27 m) and maximum (1.3 m) depths available to roots from the ESDB, which were linearly scaled by the slope. In the plain area, the value was set between 10 and 20 m to represent the thick alluvial deposits and prevailing free drainage conditions. Lastly, the maximum fractional saturated area (f_{max}) that controls runoff generation was set to zero for all grid cells containing crops due to the deep groundwater table, gentle sloping in the plain, and assuming that there are no large saturated areas in the fields and orchards. f_{max} was set to 0.16 in the remaining areas of the catchment as extracted from the global dataset. The adjusted parameters for apple were used as described in Section 2.3.1 while a separate parameter set was used for cherries to account for the earlier start of the growing season and harvest, and lower productivity as compared to apples. For the sake of consistency, parameters for winter wheat and potato were also modified based on Boas et al. (2021) with minor adjustments to growing seasons to account for the local climate (Dercas et al., 2022; FAO, 2023).

For the model spin-up, the available global GSWP3 v1 atmospheric forcing data set providing data from 1901 to 2010 at a three-hourly temporal and 0.5° spatial resolution was used (Lange & Büchner, 2020). The model was spun-up for 720 yrs until equilibrium for soil carbon and nitrogen pools, soil water storage, and other ecosystem variables was reached for all land uses in the catchment. For the remaining simulations, the model was forced with a 7 yr time series obtained from the observational data of meteorological stations CS1, CS2 (2016–2022), and CS3 (2018–2022) in the study area as well as from the two Atmos41 stations in orchard S09 and S10 (2021–2022) (Figure 1). The data was spatially interpolated to the same resolution as the surface data using inverse distance weighting. The interpolation of precipitation and temperature included a weighting factor for elevation variation using a linear correlation between station elevation and mean annual station precipitation and temperature, respectively, as described in Panagoulia (1995). Another short spin-up period of 3 yrs was performed as the orchards had just reached their maximum lifespan before orchard rotation is initiated and new seedlings need a couple of years to reach the full productivity level (Dombrowski et al., 2022).

3.3. Simulation Scenarios

A set of 1D simulations was performed to examine the effect of the irrigation parameters ψ_{target} and f_{thresh} on different aspects of the local irrigation schedule based on orchard S09 and year 2021. For ψ_{target},11 values between −20 and −1,500 kPa were tested while 15 values between zero and one were tested for f_{thresh}. The parameter set that best approximated the observed irrigation schedule and amount was chosen to adjust the irrigation routine for the subsequent simulation of the orchards. By directly applying irrigation water to the ground surface, CLM5 assumes an irrigation efficiency of 100% which is hardly achieved in sprinkler irrigation (Gilley & Watts, 1977). Based on direct observations in the studied orchards, we therefore assumed that only 75% of the water volume measured by the hydrometers reached the ground surface, while the rest is lost through interception, transpiration of the grass cover in the orchard alleys, and leakages in the pipe system. Therefore, the irrigation parameters of the CLM5 irrigation routine were calibrated to the irrigation amount that is assumed to reach the ground surface to allow for the most realistic comparison of observed and simulated SM dynamics. Consequently, simulated irrigation amounts throughout the manuscript represent only 75% of gross irrigation requirements.

To assess how well CLM5-FruitTree can represent soil moisture dynamics and crop growth in the study area, 1D simulations were performed in orchards S09 and S10 for the growing seasons 2021 and 2022. Two model set-ups were tested: the first used the current CLM5 irrigation routine with the adjusted parameterization, while the second set-up used the novel irrigation data stream to prescribe the observed irrigation. Similarly to the adjusted irrigation routine, we used 75% of the water volume measured by the hydrometers as input to the irrigation data stream. Modeling results were compared to observed SM and tree transpiration at a daily time step as well as crop yield and development. Pearson's r (r), the root mean square error (RMSE) and the percent bias (%bias) were calculated for statistical model evaluation.

For the regional case, we conducted three simulation experiments to test different irrigation scenarios. Regional data on irrigation outside the instrumented orchards S09 and S10 was not available. Thus, the model was run using

the CLM5 irrigation routine with the same parameterization that was used for the point scale simulations, in the following considered the full irrigation scenario (FI). Based on this scenario, two deficit irrigation scenarios were created for both apple and cherry orchards with 75% and 50% of full irrigation (DI75 and DI50, respectively) using the novel irrigation data stream. All scenarios were run over the same 7 yr period (2016–2022). To investigate the differences between irrigation scenarios, multi-year averages and seasonal dynamics of irrigation, SM, crop growth or yield, and crop water use efficiency (CWUE) were calculated and compared. In this study, CWUE was defined as the amount of yield produced per unit volume of water consumed (Ibragimov et al., 2007):

$$CWUE = \frac{Y}{ET} \tag{5}$$

where Y is crop yield in t ha^{-1} and ET is crop evapotranspiration in mm.

4. Results

4.1. Field-Scale Simulations

4.1.1. Effect of Irrigation Parameters on Irrigation Schedule

The CLM5 irrigation routine can be adjusted in two ways to represent an observed irrigation schedule, by Equation 1 adapting ψ_{target} or Equation 2 tuning the f_{thresh} parameter. Figure 3 shows the effect that different values of these two parameters have on several aspects of the simulated irrigation (e.g., start of irrigation period, number of irrigation events, irrigation frequency) as well as on SM and crop yield for orchard S09 and the year 2021. In both cases, a lower parameter value results in a later onset of irrigation, fewer irrigation events and lower total irrigation amounts. However, the parameters have different effects on irrigation frequency, whereby smaller values of f_{thresh} result in less frequent irrigation events while the irrigation volume per event increases (Figure 3). Changing ψ_{target}, on the other hand, has little effect on the irrigation frequency and volume. SM in the upper 50 cm of soil increases with increasing values of both parameters. The increase is exponential for ψ_{target} with values ranging between 0.195 and 0.275 cm^3 cm^{-3} and almost linear for f_{thresh} with a somewhat smaller range. Consequently, varying ψ_{target} has a more pronounced effect on yield compared to f_{thresh} for the investigated range of parameter values.

Based on the analysis in Figure 3, we set f_{thresh} to 0.7 while leaving ψ_{target} at its default value of −34 kPa for the model run using the CLM5 irrigation routine to approximate the main characteristics of the observed irrigation schedule (approximately weekly irrigation events averaging 26 mm per event, starting mid-May).

4.1.2. Soil Moisture and Matric Potential Dynamics

Figures 4 and 5 show the SM time series at 5, 20, and 50 cm depth and SMP at 20 cm depth for S09 and S10, respectively. The interquartile range (Q_{25}-Q_{75}), calculated from 24 measurements (12 nodes with two profiles each) for every depth, shows considerable variability in SM, especially in S10 and at 50 cm depth. This reflects the high heterogeneity of soil texture and gravel content that was observed during soil sampling. When comparing the observed SM dynamics in the two orchards, S09 showed 4–12 vol% higher SM on average compared to S10 throughout the measurement period. The soil textural analysis of both orchards clearly showed a higher clay and organic matter content, and lower gravel content in S09 compared to S10 (Table 1). Frequent rainfall during the winter months (631 and 606 mm in 2021 and 2022 respectively) kept the soil close to saturation with average SMP around −8.5 kPa in both orchards. Starting in April the soil gradually became drier causing a steep decline in SMP to around −500 kPa (S09) and −300 to −400 kPa (S10) by mid-May. The decline resulted from low rainfall amounts and increased evaporation demand along with water consumption from the grasses in the alleys and the fruit trees. During both seasons, the farmer irrigated every 5–7 days starting mid-May through October. Irrigation amounts per event varied strongly and averaged 14 and 25 mm in S09 and S10 respectively (upper panel of Figures 4 and 5). Irrigation increased SM by up to 10 vol% in the top 5 cm and about 5 vol% at 50 cm depth.

In addition to the observations, the simulation results using both the current CLM5 irrigation routine and the novel irrigation data stream are shown for the corresponding CLM5 soil layers in Figures 4 and 5. Table 4 lists the model quality parameters used to evaluate the simulation results. The model simulations outside the irrigation season, using either irrigation approach, corresponded well to the observed SM in S09. However, in S10, CLM5

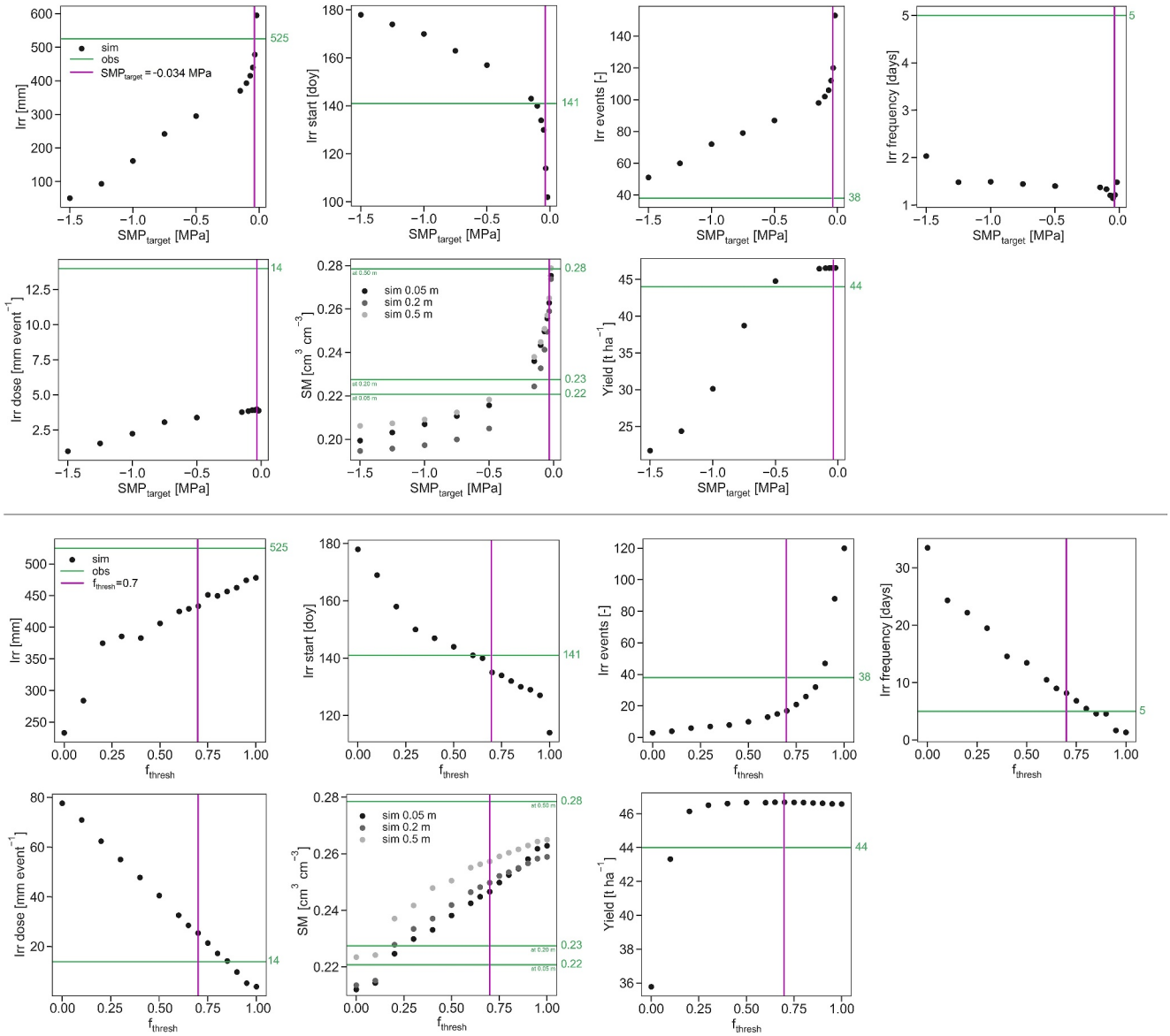

Figure 3. Effect of irrigation target soil matric potential (ψ_{target}) and irrigation threshold fraction (f_{thresh}) on total irrigation amount (Irr), irrigation starting date (Irr start), number of irrigation events (Irr events), irrigation frequency (Irr frequency), irrigation dose per event (Irr dose), soil moisture (SM) at 5, 20, and 50 cm depth, and yield. Shown are yearly average values for S09 and the year 2021.

overestimated SM in the soil profile by on average 4.5–7.3 vol%. The observed differences in SM between both orchards were not captured by the model where SM values in S10 were only 1–2 vol% higher. In April and May, just before the start of the irrigation season, the simulations showed the strongest deviation from observed values for both orchards as the soil drying was much less pronounced in the simulations. During the irrigation season, the adjusted CLM5 irrigation routine could only partially reproduce the observed irrigation schedule and SM dynamics compared to using the irrigation data stream. Nevertheless, both irrigation approaches showed fluctuations of similar magnitude compared to the observed values in the upper soil. Less dynamics than observed were simulated at 50 cm depth for both irrigation approaches and both orchards. The wet bias in S10 was still persistent throughout the profile for the simulation using the novel irrigation data stream while simulated SM based on the adjusted CLM5 irrigation routine dropped to the range of observed values (Figure 5).

Simulated and observed total yearly irrigation were similar in S09 with the observed irrigation reaching the soil surface (75% of total measured irrigation) being 433 and 458 mm and simulated amounts being 425 and 439 mm

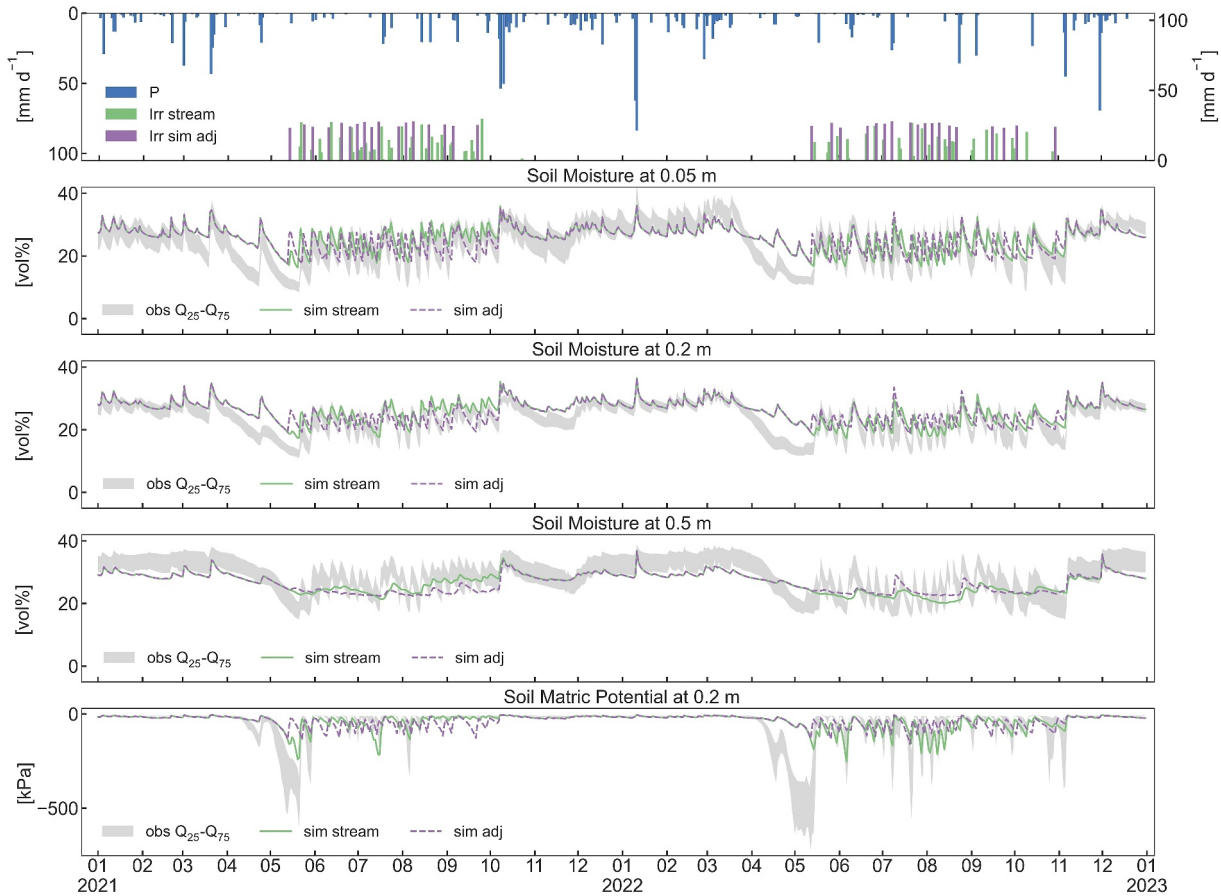

Figure 4. The upper panel shows precipitation, and observed and simulated irrigation for orchard S09 in mm d^{-1}. The central panels show observed soil moisture (SM) as interquartile range between the 25th and the 75th percentile from 24 measurements, simulated SM using the adjusted CLM5 irrigation routine and the novel irrigation data stream at 5, 20, and 50 cm depths. The bottom panel shows observed interquartile range and simulations using the two irrigation approaches of soil matric potential (SMP) at 20 cm depth for orchard S09 for 2021 and 2022.

for 2021 and 2022, respectively. In S10, observed irrigation amounts were considerably higher than in S09, which could be expected considering the lower observed SM in S10. Compared to the observed 706 and 586 mm, for 2021 and 2022, respectively, the model applied only 393 and 388 mm, which is a result of the simulated wet bias.

4.1.3. Tree Transpiration and Fruit Harvest

The comparison of measured sapflow with simulated transpiration expressed as water consumption per tree is presented in Figure 6. Observed sapflow varied significantly between different trees resulting in large interquartile ranges. The two model runs showed no difference in simulated tree transpiration despite the difference in irrigation amount and timing. In 2021, CLM5 showed higher values and a slight shift in the seasonal dynamic as a result of a too early onset of leaf development compared to the observed values (LAI_{sim} in Figure 6). Simulated leaf duration and total transpiration agreed well with the measurements in 2022. Tree transpiration peaked in July with a measured monthly average of 12.5 (2021) and 20.2 L tree^{-1} day^{-1} (2022) and simulated values of 25.1 (2021) and 24.5 L tree^{-1} day^{-1} (2022). The better agreement between simulated and observed values in 2022 followed a reinstallation that was performed after partial sensor failure and unreliable measurements that resulted in data gaps for the 2021 growing season. The 2021 data should therefore be handled with care when interpreting absolute values. Simulated maximum leaf area index (LAI) was reached in early July. Full canopy cover in the orchards occurred in the second half of June, so slightly earlier, based on visual inspection of the phenocam pictures (data not shown). Simulated leaf area and hence transpiration fell to zero by December, which broadly agreed with observed sapflow and leaf senescence deduced from the phenocam images.

10.1029/2023WR036139

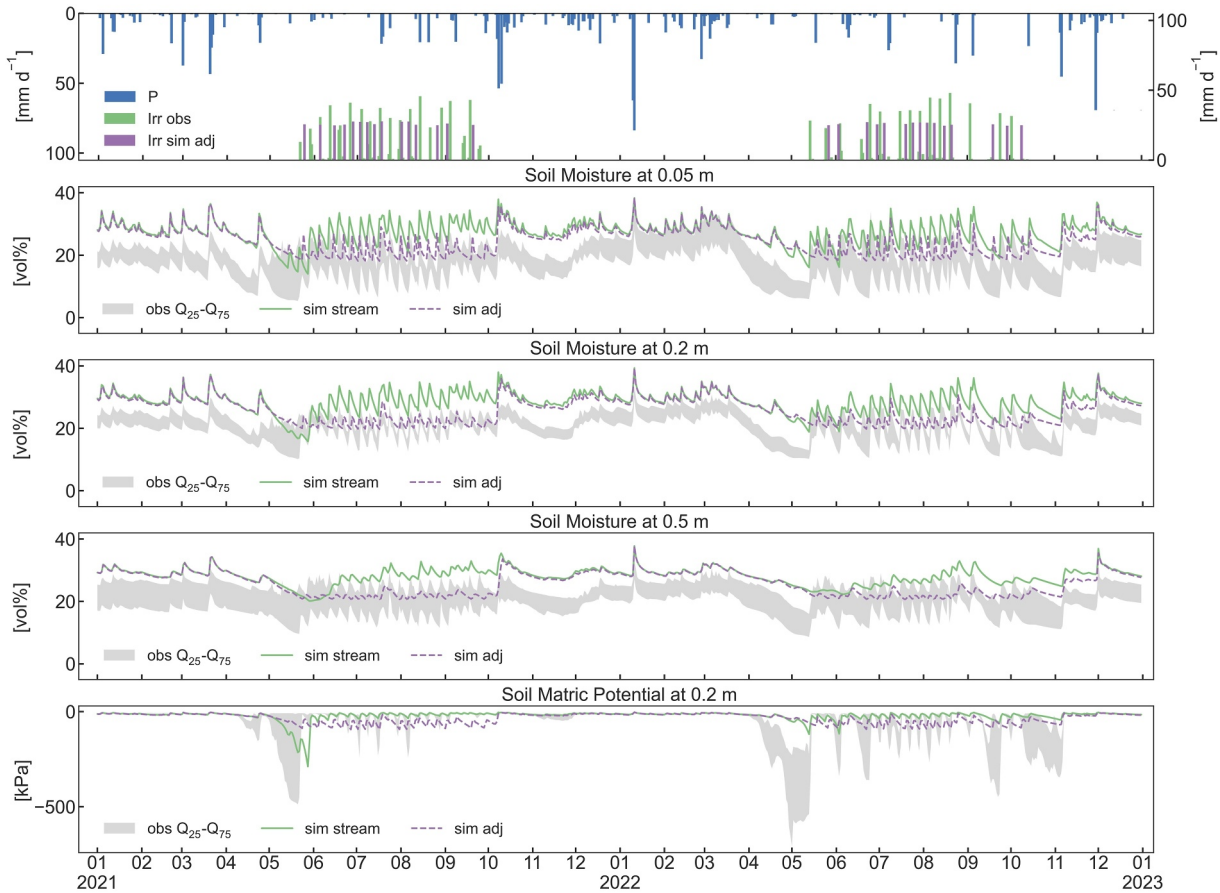

Figure 5. The upper panel shows precipitation, and observed and simulated irrigation for orchard S10 in mm d^{-1}. The central panels show observed soil moisture (SM) as interquartile range between the 25th and the 75th percentile from 24 measurements, simulated SM using the adjusted CLM5 irrigation routine and the novel irrigation data stream at 5, 20, and 50 cm depths. The bottom panel shows observed interquartile range and simulations using the two irrigation approaches of soil matric potential (SMP) at 20 cm depth for orchard S10 for 2021 and 2022.

Table 4
Pearson's r (r), Root Mean Square Error (RMSE) and Percent Bias (%Bias) for Soil Moisture (SM) at 5, 20 and 50 cm Depth and Soil Matric Potential (SMP) at 20 cm Depth in Orchards S09 and S10 Simulated Using the Novel Irrigation Data Stream

		S09			S10		
	Soil depth (m)	r	RMSE (vol%)	%Bias	r	RMSE (vol%)	%Bias
Whole year 2021/2022	0.05	0.88/0.81	3.97/3.89	13.13/8.18	0.77/0.83	9.55/8.08	50.21/39.89
	0.2	0.88/0.86	3.10/3.23	10.14/9.26	0.75/0.84	8.18/7.68	37.30/35.55
	0.5	0.78/0.80	3.08/3.49	−6.60/-6.63	0.56/0.72	8.06/7.65	37.48/36.13
	SMP (kPa)	0.82/0.63	56.25/89.67	−27.54/-37.14	0.62/0.75	41.65/122.41	−35.44/-76.14
Irrigation season 2021/2022	0.05	0.86/0.74	3.85/3.02	15.47/4.30	0.70/0.83	5.13/8.43	21.13/45.60
	0.2	0.84/0.77	3.00/2.84	10.86/8.10	0.67/0.77	2.3/7.70	4.51/37.32
	0.5	0.48/0.27	3.12/3.74	−6.27/-6.14	0.25/0.45	1.73/7.10	−0.74/33.74
	SMP (kPa)	0.73/0.64	46.61/61.36	−11.08/-7.54	0.65/0.66	52.04/98.86	−81.11/-72.95

Note. The first number refers to 2021 and the second number to 2022. Statistics were calculated for the whole year and for the irrigation season only (21st May to 25th Sep for 2021; fifteenth May to 10th Oct and fourteenth May to 2nd Oct for S09 and S10, respectively, in 2022).

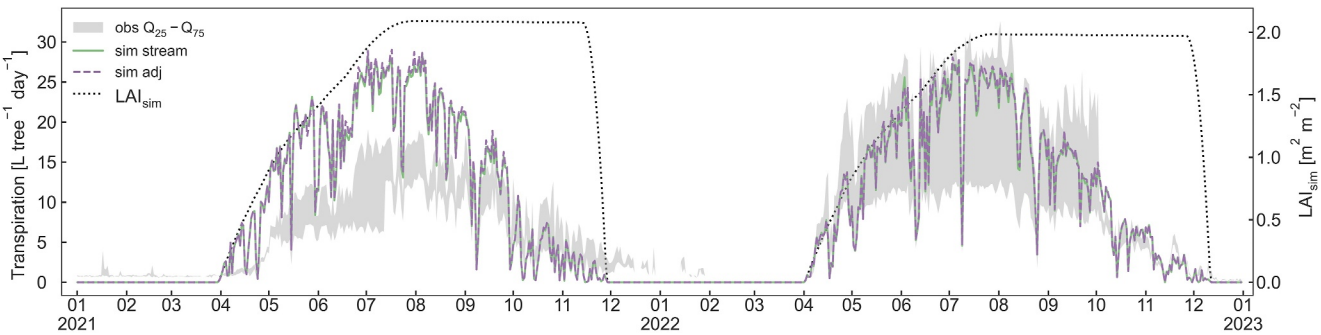

Figure 6. Whole tree transpiration estimated from the sapflow sensors in orchard S10 together with simulated transpiration expressed in liters per tree and day, and simulated leaf area index (LAI_{sim}) for 2021 and 2022.

Generally, fruit harvest in the orchards was performed between seventeenth of August and 30th of October in a first and second harvest for most varieties. Due to very low apple quantity, harvest in 2022 occurred in a single harvest between 1st Sep and 15th Nov depending on variety. Simulated harvest in 2021 occurred on twelfth and 18th Sep for S09 and S10 respectively, and a few days earlier in 2022. The two simulation runs using either the adjusted CLM5 irrigation routine or the novel irrigation data stream showed no difference in harvest amounts. In 2021, simulated yield was close to the observed values while the exceptionally low yield in 2022 was not captured by the simulations (Table 5). Visual inspection of the phenocam images showed significantly less flowers on the trees in 2022 compared to 2021 (data not shown). No extreme weather conditions were observed during the winter 2021/2022 that could explain the reduced flowering. Other possible reasons for the low number of flowers and hence low yield in this year may be related to alternate bearing of the varieties or other factors (e.g., plant physiology or traits, pest and disease or certain management practices) that are not included in the model.

4.2. Regional Simulations

4.2.1. Irrigation Signature in the PHO

Figure 7 shows simulated seasonal mean SM and sum of evapotranspiration (ET) within the PHO averaged over the 7 yr period. Depicted values represent grid cell averages, meaning they are the weighted average of all land uses in a given cell. During the winter months and into spring, SM is high throughout the catchment, but with a declining gradient along the North-South axis from the mountainous part down to the plain. ET in the catchment is low during winter but starts to increase in spring, revealing a discernible pattern attributed to differences in land use (Figure 1). During the summer months, ET reaches its peak, displaying a distinct irrigation signature with significantly higher ET values of 293 mm on average over irrigated land, as opposed to 214 mm on average in the rest of the catchment. The pattern persists throughout autumn and is also evident in summer and autumn SM, albeit less pronounced due to the lower productivity of rainfed vegetation, resulting in reduced water uptake from the soil. The subsequent analysis will focus exclusively on the irrigated land, more specifically on apple orchards, as they account for 91% of the total irrigated area.

Table 5
Observed and Simulated Apple Yield in t Ha^{-1} for Orchards S09 and S10 for 2021 and 2022

	Yield in S09 (t ha^{-1})		Yield in S10 (t ha^{-1})	
Year	Obs	Sim	Obs	Sim
2021	44	47	47	51
2022	16	49	11	50

4.2.2. Simulated Spatial Patterns

Figure 8 shows average and standard deviation of the 7 yr simulation period for irrigation, SM, yield, and CWUE for all apple orchards in the PHO, between 2016 and 2022. Modeling results show a clear spatial pattern that is driven by climatic conditions following the topographic gradient (Figure 1) on the one hand and soil characteristics on the other hand (Figure 2). Average yearly irrigation requirements range between 400 and 450 mm in the plain. The highest values are found in the southeast while considerably lower values occur at higher altitudes in the northern part of the catchment (<200 mm). Harvest values show a similar pattern because cooler temperatures and lower incoming radiation in the northern part of the catchment result in lower crop

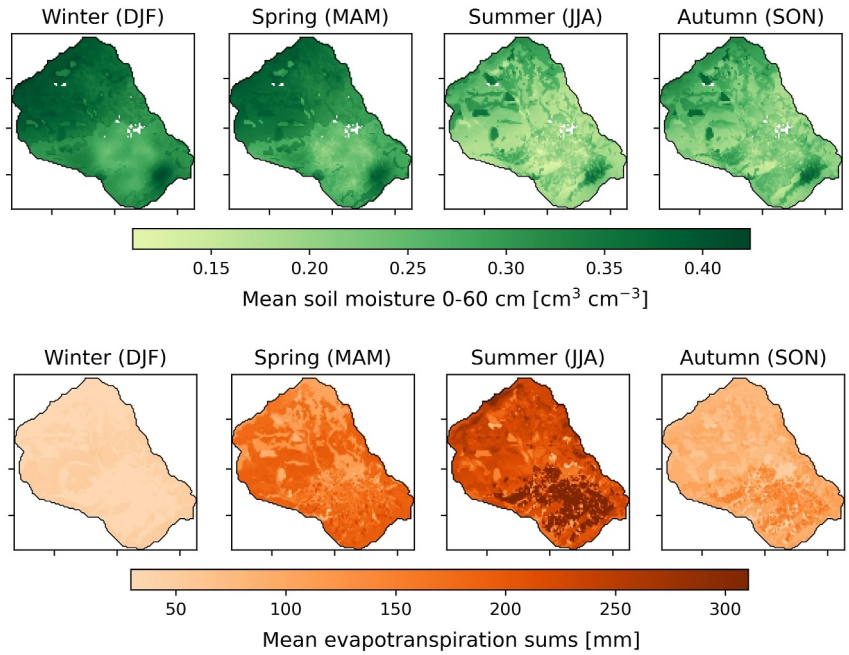

Figure 7. Seasonal mean soil moisture, and evapotranspiration sums in the PHO catchment, averaged over the period 2016–2022.

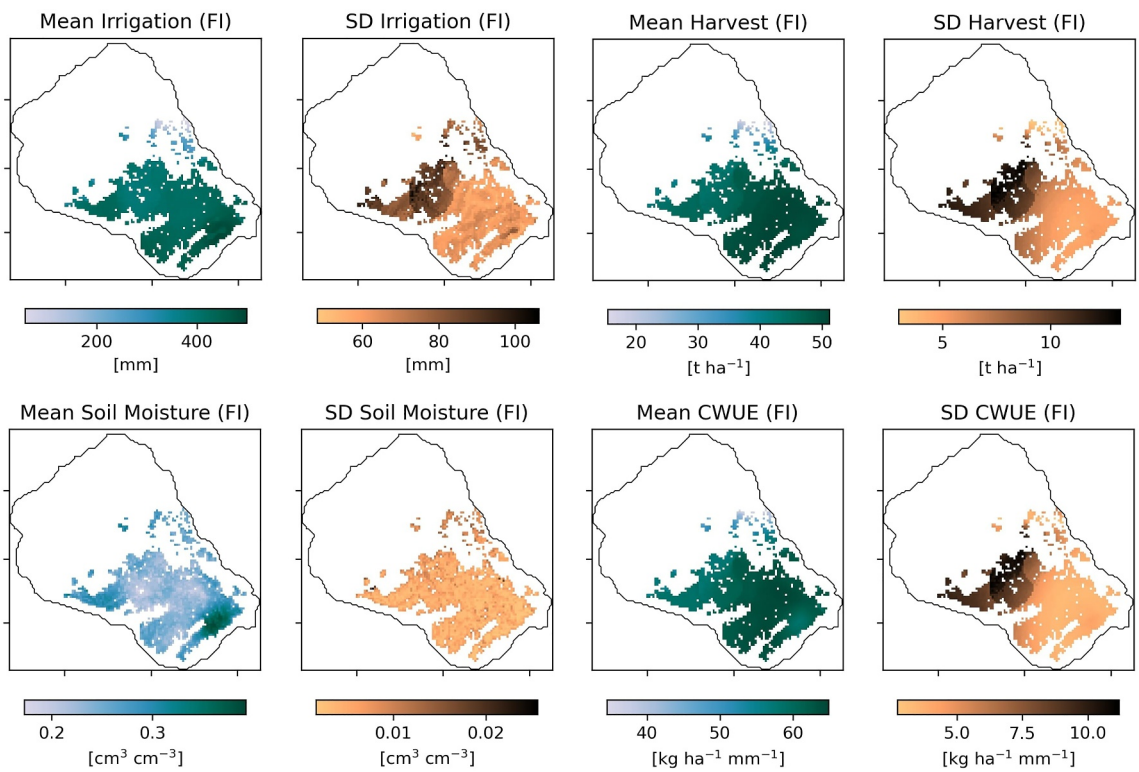

Figure 8. Mean and standard deviation (SD) of average yearly irrigation, soil moisture in the root zone (0–60 cm), harvest, and crop water use efficiency (CWUE) for apple orchards within the PHO between 2016 and 2022 under full irrigation (FI).

productivity and thus smaller yields (16–38 t ha^{-1}) compared to the plain where yields are around 50 t ha^{-1} without much spatial variability. In addition to lower crop productivity and thus lower crop water demands, spatial variability in irrigation requirements results from the higher precipitation in the upper parts of the catchment that further reduces the need for irrigation as well as soil textural differences. The latter is most evident in the southern part of the catchment where the higher clay content and the consequently higher water holding capacity of the soil result in increased evaporation (not shown). This in turn generates a greater irrigation demand resulting in slightly lower CWUE of orchards planted on these soils. Soil textural differences are also reflected in the SM plot where areas with a higher percentage of clay or organic matter show higher SM values than areas with sandier soils or soils that are lower in organic matter. CWUE ranges from 57 to 65 kg ha^{-1} mm^{-1} in the plain to 35–45 kg ha^{-1} mm^{-1} in the northern part of the catchment and largely reflects the spatial patterns of irrigation and harvest whereby high irrigation requirements and low harvest lead to low CWUE. Inter-annual variability (standard deviation plots) within the catchment shows similar patterns for irrigation, harvest, and CWUE and is higher in the northwestern part of the catchment. The higher variability was driven by local temperature differences in some years that delayed the onset of the growing season up to 14 days compared to the remaining orchards. Inter-annual variability of SM is generally low without a distinct spatial pattern.

4.2.3. Effect of Irrigation Deficit Scenarios

The effect of deficit irrigation on total irrigation amounts, harvest, and CWUE of apple orchards in the PHO for the moderate irrigation deficit scenario, DI75, and the more severe deficit scenario, DI50, are shown in Figure 9. Yield differences between the FI and the DI75 scenario are almost negligible, ranging from a decline of maximum 3 t ha^{-1} (5%) to even slight increases in yield. However, the DI50 scenario resulted in a clear decline of simulated yield with up to 12 t ha^{-1} corresponding to a 30% reduction in yield compared to the FI scenario. Nonetheless, orchards located at high altitudes and in the southeast on clay-rich soils are still barely affected by the higher water deficit (<5% decline in yield). Overall, annual water savings are highest in the plain, averaging 100–125 mm for DI75 and 210–250 mm for DI50. CWUE shows a differing pattern between both scenarios. While in DI75, CWUE declines slightly in the central part of the plain by around 1 kg ha^{-1} mm^{-1} (2%), there are large areas that show an increase in CWUE of similar magnitude. The decline in CWUE is concentrated on the orchards growing on soils with a high percentage of sand. For DI50, on the other hand, CWUE is almost exclusively showing a decrease of up to 8.8 kg ha^{-1} mm^{-1} (17%), though again CWUE for orchards in the higher altitudes and the ones located on soils with higher clay content are less affected.

4.2.4. Irrigation and Yield at the Inter-Annual and Monthly Scale

Yearly irrigation amounts, precipitation during the main irrigation season, and harvest averaged for all apple orchards in the PHO are shown in Figure 10. For the investigated 7 yr period, irrigation ranges between 297 and 487 mm while precipitation is around 167–322 mm from May to October. Differences in precipitation drive the inter-annual variability in irrigation requirements whereby drier summer months, such as 2019–2022, result in higher irrigation demand compared to wetter years. Yield ranges between 32 and 55 t ha^{-1}, with 2019 and 2020 being the years with the highest yields due to favorable meteorological conditions (high solar radiation and temperature). Notably, the effect of deficit irrigation on yield is strongest in these two years reducing yield by > 12 t ha^{-1} for the DI50 scenario. In contrast, both the DI75 and DI50 scenario have negligible effect on yield in the first three simulation years.

Figure 11 shows the seasonal course of irrigation, precipitation, and fruit growth in the apple orchards averaged over the PHO and the 7 yr period. The simulated irrigation season starts in April or May and lasts until October with negligible amounts still applied in November for some years. Monthly irrigation requirements increase sharply between April and June until reaching their peak in August with on average 107 mm per month. Accordingly, August is also the month in which the greatest water savings occur for the deficit scenarios. After that, irrigation declines rapidly. Fruit biomass increases steadily from April to harvest in September with faster growth occurring in the earlier months. While fruit growth is barely affected by a 25% reduction in irrigation (DI75), for the DI50 scenario it decreases sharply in August and to a smaller extent in July and September. The reduced fruit growth results in a yield loss of on average 0.5 t ha-1 for DI75 and 6.5 t ha-1 for DI50.

10.1029/2023WR036139

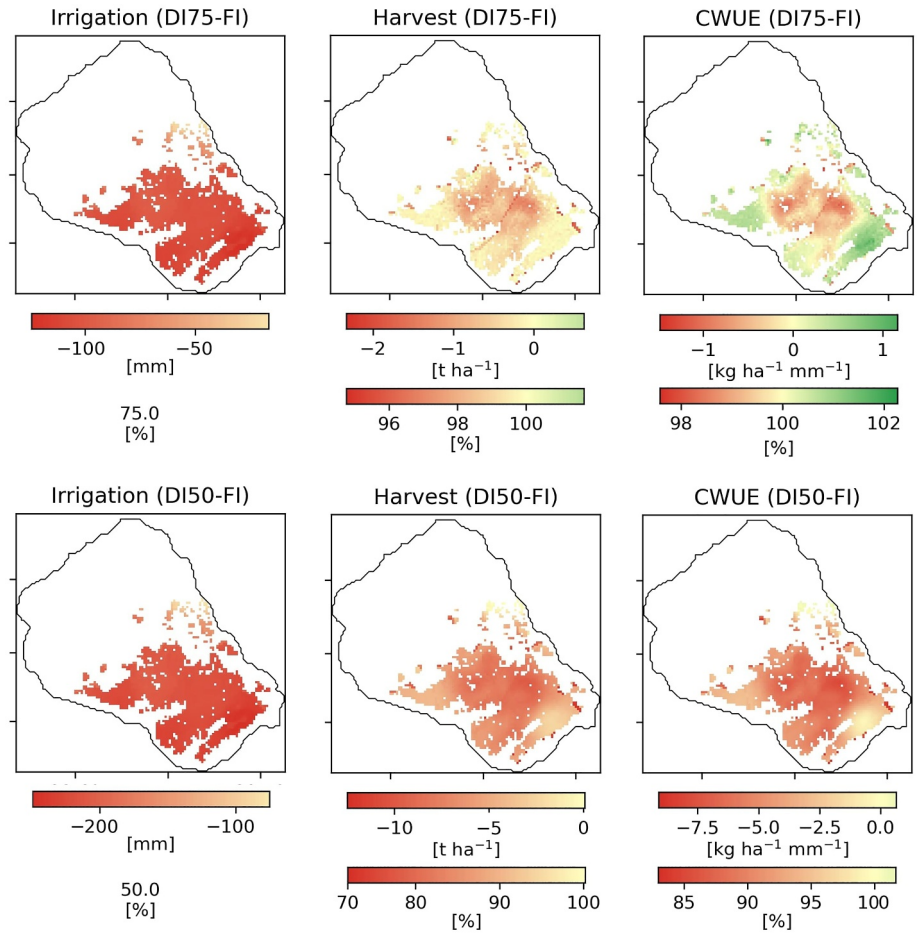

Figure 9. Absolute and relative differences in irrigation amount, harvest, and crop water use efficiency (CWUE) between the full and the 75% irrigation scenario (DI75-FI), and the full and 50% irrigation scenario (DI50-FI) for apple orchards within the PHO during the period 2016–2022.

5. Discussion

5.1. Evaluation of the CLM5 Irrigation Routine

The direct comparison of simulated SM dynamics to observed SM from a dense sensor network in two irrigated orchards gave valuable insights into model performance. Our findings demonstrate that the current CLM5 irrigation routine lacks the necessary flexibility to represent specific irrigation practices observed in the orchards. Simulated crop growth and transpiration at the orchard scale were not sensitive to the difference in irrigation amount and timing between the two model runs using the adjusted CLM5 irrigation routine and the novel irrigation data stream respectively. However, as differences between the simulated and actual irrigation practices increase, the effects may become more important especially considering runoff generation or sensible and latent heat fluxes that were not analyzed in this study. Similarly, if the irrigation is limited so that the crop experiences some degree of water stress, the timing of irrigation may become more important. This could be further tested by applying different irrigation schedules under various amounts of irrigation using the novel irrigation data stream.

Prior studies using the irrigation module in CLM were limited to calibrating the target SM or adjusting the irrigation threshold fraction to match gross irrigation requirements reported at the country or regional level, or performed no calibration at all (Felfelani et al., 2018; Leng et al., 2015; Leng et al., 2013; Zhu et al., 2020). The model, however, does not currently consider restrictions on irrigation schedule, over irrigation, or irrigation efficiency that significantly affect gross irrigation requirements as our results revealed. The novel irrigation data stream can be used to overcome some of these limitations by prescribing crop and farmer specific irrigation

10.1029/2023WR036139

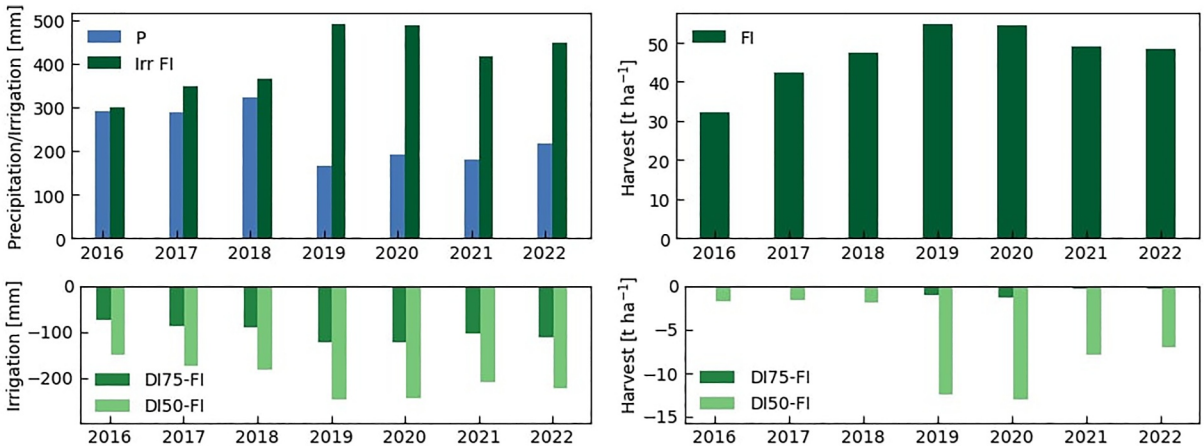

Figure 10. Yearly sum of precipitation during the main irrigation season (May-Oct), irrigation, and harvest averaged over all apple orchards within the PHO from 2016 to 2022, under full irrigation (FI) and the difference for the 75% and the 50% deficit irrigation scenarios (DI75 and DI50).

schedules and amounts. This allows investigating the irrigation-induced effects on for example, crop yield, SM, or carbon and energy fluxes under observed irrigation practices and can help to identify existing model biases by removing one possible source of uncertainty.

5.2. Model Uncertainties, Limitations and Possible Improvements

5.2.1. Parametric Uncertainty

SM dynamics outside the growing season were well reproduced by CLM5, indicating that the model was able to capture infiltration and soil water redistribution in the studied orchards under natural conditions. However, the significant SM bias in S10 suggests structural and parametric uncertainty in the estimation of soil hydraulic properties, probably due to inappropriate pedotransfer functions implemented in CLM5 (X. Han et al., 2015). Gao et al. (2021) found that poor performance of CLM5 in reproducing observed root zone soil moisture was mainly due to uncertainty in porosity estimates. In addition, a high content of rock fragments, which is typical of many Mediterranean soils (Nijland et al., 2010; Poesen & Lavee, 1994; Zalidis et al., 2002), can strongly influence the SM regime through non-linearity in soil hydraulic conductivity and by reducing the soils' effective porosity (Angulo-Jaramillo et al., 1997). For this reason, most pedotransfer functions fail to correctly reproduce the hydraulic properties of stony soils (Nasri et al., 2015), which likely led to biases in simulated SM in S10. Further investigation of the results would be needed to confirm this hypothesis, for example, data assimilation of observed soil variables could be used to optimize soil hydraulic parameters (Strebel et al., 2022). In both orchards, the

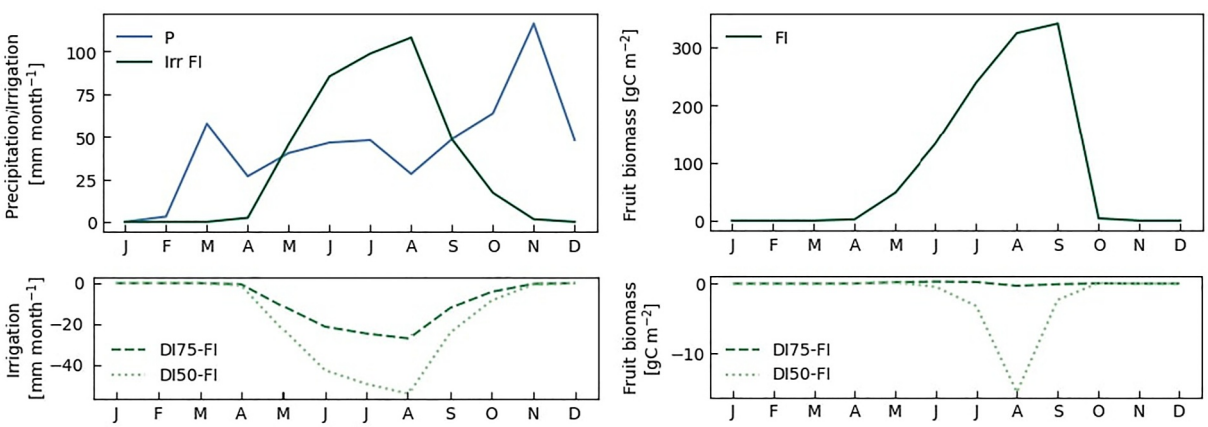

Figure 11. Seasonal pattern of monthly precipitation, irrigation, and fruit biomass averaged over all apple orchards within the PHO and the period 2016–2022, under full irrigation (FI) and the difference for the 75% and the 50% deficit irrigation scenarios (DI75 and DI50).

simulations showed a lower simulated SM dynamic in 50 cm depth, which could be the result of uncertainties in the rooting distribution and thus root water uptake within the soil profile. The current parameterization of the vertical discretization of root fraction results in a rather shallow profile while deeper roots may still contribute to root water uptake in the studied orchards. Shrestha et al. (2018) encountered a similar issue when analyzing root zone SM on a grassland site using CLM3.5 and were able to improve simulated SM dynamics by increasing the root fraction in deeper layers. This may help to improve the simulated SM dynamics at 50 cm on our study sites.

The sensitivity experiments performed using two parameters of the CLM5 irrigation routine (Figure 3) and the results from the irrigation scenarios revealed relatively low sensitivity of crop yield to reduced irrigation (Figure 9). The new plant hydraulic stress (PHS) routine introduced by Kennedy et al. (2019) advanced the physical basis for hydraulic stress in the model, but there is large uncertainty in its parameterization. Currently PHS parameters are generic for all crops while it is well established that reactions to water stress and levels of SM depletion differ amongst different crops and crop varieties (Budak et al., 2013; Chaves et al., 2003). Consequently, water stress for apple trees may not be accurately represented in the model, which limits its ability to reliably determine optimal irrigation amounts or assess the trade-off between yield loss and water savings under the tested deficit irrigation scenarios. To better quantify the model performance and find the most suitable parameters for apple orchards, comparison of simulations to observations from stressed and non-stressed crops would be necessary. Additionally, sensitivity analysis of PHS parameters, which was out of the scope for this paper, could help to better constrain these model parameters.

5.2.2. Crop Representation

The PHO catchment is characterized by a diversity of small-scale farm holders resulting in considerable heterogeneity in management practices, which can be only partially captured by the model. While simulated yield was close to observations during a "good" year for the point-scale simulations, according to Mattas et al. (2019) average Greek apple production in 2016 was only ∼23 t ha^{-1}. This suggests a great variability in orchard productivity, apple cultivars, or type of end product (e.g., apples for direct consumption or for juice) which would necessitate the inclusion of additional crop types and management practices in CLM5. In striving for global applicability, CLM5 and other LSMs face constraints in computational resources and often insufficient observational data to parameterize additional crop types, which results in biases in certain regions, while others are more accurately represented (Lombardozzi et al., 2020). In our case, the model demonstrated a strong correlation of yield and irrigation with the climatic gradient induced by the topography in the PHO, indicating a high sensitivity to model forcing data. The large simulated differences in yield between orchards in the plain (∼50 ton ha^{-1}) versus the higher altitudes (as low as 16 ton ha^{-1}) may however be exacerbated, as CLM5 employs a single set of parameters for a given crop across diverse geographies and climates. In reality, various cultivars of the same crop type, along with plant physiological adaptations to their environments, can lead to comparable productivity levels despite variations in climatic conditions. This phenomenon is evident in the cultivation of numerous crops, including apples, across climates on a global scale (Sherman & Beckman, 2002). The issue has been addressed by Lombardozzi et al. (2020) who recommended further developments in CLM5 to improve phenological triggers and agricultural management, and to include different cultivars. In the future, the incorporation of additional satellite-derived crop data, advanced parameterizations, or the use of crop calendars to constrain these models may help reduce some of the biases (Pongratz et al., 2018; Yao et al., 2022; Z Zhang et al., 2020).

At the orchard scale, we found discrepancies between observed and simulated SM during the growing season that suggest limitations specific to the current representation of orchards. As CLM5 does not allow intercropping, the actively growing grass cover in the orchard alleys is not included in the CLM5-FruitTree sub-model (Dombrowski et al., 2022). Consequently, our simulations do not account for the additional root water uptake and transpiration as well as interception of the irrigation water from the grasses. The former may explain the smaller simulated decline in SM early in the season compared to the observations, while we considered the latter to some extent by assuming a reduced irrigation efficiency of 75%. In doing so, we did however neglect the additional ET flux. Yao et al. (2022) developed and tested different irrigation techniques in CLM5 and found an increase in canopy evaporation through increased interception for their implementation of sprinkler irrigation. However, the overall impact on ET and total applied irrigation remained small compared to the control run using the standard CLM5 irrigation. More importantly, accounting for conveyance and application losses would increase the simulated irrigation amount and could lead to more realistic irrigation values (Yao et al., 2022).

Despite these limitations, and though we could not validate the simulation of crop yield and irrigation requirements in the PHO catchment due to the lack of observational data, the reasonable modeling results at the orchard scale give some confidence in the robustness of the regional simulations.

5.3. Implications for Irrigation and Water Resources Management Using CLM5

The analysis performed in this study examined the current ability and potential of applying CLM5 for irrigation and water resources management at local and regional scales. Model application at the orchard scale revealed the importance of careful calibration of the irrigation routine next to soil and crop-specific parameterization to approximate the observed irrigation schedule and soil moisture dynamics. However, the suitability of CLM5 for field-scale irrigation management and yield optimization is currently limited by its simplified crop and management representations and by the uncertainties in accurately capturing the relationship between plant water stress and yield. For these applications, specialized agricultural models are likely to be better suited. Nevertheless, field-scale application of LSMs such as CLM5 as performed in this study are highly relevant and necessary for a detailed validation and calibration of the models and to ensure the reliability of further predictions at the regional scale and beyond. Additionally, these studies can help to identify areas of uncertainty and necessary model improvements, as discussed above.

At the regional scale, the model application provided insights into the drivers of irrigation demand such as meteorological conditions, soil type, and irrigation requirements. For most part of the investigated catchment, simulated CWUE and yield were hardly affected when irrigation was reduced to 75%, while a reduction to 50% led to a decrease in yields of up to 30%. There are two possible explanations for the interpretation of these results. First, the effect could be caused by poorly calibrated parameters of the PHS routine as discussed in Section 4.2.1 resulting in a low sensitivity of crops to water stress. Alternatively, the negligible effect of DI75 could suggest that the current irrigation applied by the local farmers (FI scenario) provides more water than what the orchards need. Thus, DI75 could be closer to optimal irrigation with maximized yield and minimized water consumption as opposed to the over-irrigation in the FI scenario. This could result in considerable water savings of up to 125 mm per year, with little to no effect on apple yields. Tsakmakis et al. (2023) reached similar conclusions and, by using modeled crop evapotranspiration in the same orchards and for the same years, estimated that applied irrigation might be reduced from 15 up to 50% compared to observed amounts. Similarly, Li et al. (2018), who used CLM to schedule irrigation in a citrus orchard in Spain, suggested that 24% less irrigation could be applied compared to the farmers' practices. It has in fact been noted that farmers tend to over-irrigate when water availability is not a constraint and water prices are low (Latinopoulos, 2005). Despite the uncertainty in plant water stress representation in CLM5, a certain water saving potential can thus be expected for the catchment.

Beyond the relatively uncertain implications of the various irrigation scenarios on crop yield, the regional simulation revealed the periods of peak irrigation demand and areas of high vulnerability to water stress. This is relevant as it is expected that competition between different water use sectors will become a key issue and will require local governments and decision makers to design appropriate water allocation plans. As this includes considering the interactions of irrigation and freshwater availability and its' impact on water resources, energy fluxes, and climate, LSMs present powerful tools for such integrated assessment. While the use of the irrigation data stream at larger scale is currently hampered by the limited availability of precise information on irrigation practices in most areas (Felfelani et al., 2018), it can serve as a valuable tool to investigate the modeled effect of different irrigation schedules and water availability scenarios to assess irrigation-related policies and their implications on water availability and ecosystem functioning. Additionally, the growing inclusion of irrigated land in long-term observational networks like TERENO will likely benefit model development in the future (Zacharias et al., 2024).

In order to further improve the suitability of CLM5 for this kind of application, model development should focus on including irrigation efficiency and moving to crop-specific or spatially explicit representation of irrigation parameters. Also constraining irrigation by water availability will be essential for realistic irrigation representation. Lastly, the coupling of LSMs with hydrologic (e.g., groundwater) or atmospheric models would allow to study the interactions and feedback mechanisms between these system components in a more comprehensive way.

6. Conclusions

This study assessed the ability of the CLM5-FruitTree sub-model to represent field-scale irrigation practices in fruit orchards in a small Mediterranean catchment and explored the extent to which CLM5 could aid irrigation and water management at regional scale. After calibration, the current CLM5 irrigation routine could only partially reproduce observed irrigation practices. Therefore, an irrigation data stream that directly prescribes measured irrigation data was implemented to assess the model performance against observed SM dynamics, transpiration, and yield. While SM dynamics in the two studied apple orchards were mostly well captured by the model, we did find some discrepancies between observed and simulated variables that were related to uncertainties in soil hydraulic parameters and limitations in the crop representation. While such model deficiencies currently limit the ability of CLM5 for field-scale irrigation optimization, the simulations revealed areas for further model improvement that can increase model performance at regional scale and beyond.

At regional scale, we could simulate different irrigation scenarios through the novel irrigation data stream. The modeling results, suggested potential water savings under reduced irrigation and identified periods of peak irrigation demand and areas of high vulnerability to water stress. Apart from these results, clearly regional applications of LSMs such as CLM5 can reveal the effect of irrigation on water availability, energy fluxes, and climate, making them a powerful tool for assessing the broader implications of irrigation and designing water allocation plans. To enhance the suitability of CLM5 for such applications, future model development should focus on including irrigation efficiency, more diverse irrigation schedules and water availability next to coupling with hydrologic or atmospheric models to study system interactions and feedback mechanisms.

Data Availability Statement

The CLM5-FruitTree sub-model used in this work is freely available in Dombrowski (2022). The irrigation data stream implementation is available in Swenson (2023). Climate data from climate stations CS1, CS2, and CS3 from the TERENO sites around Agia (TERENO ID: AGIA_K_001, AGIA_K_002, AGIA_CK_003) are freely available via the TERENO data portal (TERENO, 2023a; TERENO, 2023b; TERENO, 2023c). Data collected from the two apple orchards S09 and S10 is available via the TEODOOR database in Dombrowski and Bogena (2023). Data analysis was performed in Python version 3.10.4 (PythonSoftwareFoundation, 2023) and figures were made with Matplotlib version 3.5.2 (Caswell et al., 2022). The map overview was created with QGIS version 3.12.3 (Dawson et al., 2022).

Acknowledgments
This research received support from the ATLAS project, funded through the EU's Horizon 2020 research and innovation program, under grant agreement No. 857125. Further support was received from the German Research Foundation (DFG) through the project 357874777, which is part of the research unit FOR 2694 Cosmic Sense as well as through the PhenoRob project as part of Germany's Excellence Strategy - EXC 2070–390732324. Additional support was received from TERENO (Terrestrial Environmental Observatories) of the Helmholtz Association of National Research Centers (HGF), Germany. Furthermore, this work was in part supported by the National Center for Atmospheric Research (NCAR), which is a major facility sponsored by the NSF under Cooperative Agreement 1852977. Simulations were conducted using computing resources from the supercomputers JURECA and JUWELS from Jülich Supercomputing Centre (JSC). Open Access funding enabled and organized by Projekt DEAL.

References

Angulo-Jaramillo, R., Thony, J., Vachaud, G., Moreno, F., Fernandez-Boy, E., Cayuela, J., & Clothier, B. (1997). Seasonal variation of hydraulic properties of soils measured using a tension disk infiltrometer. *Soil Science Society of America Journal*, *61*(1), 27–32. https://doi.org/10.2136/sssaj1997.03615995006100010005x

Ballabio, C., Panagos, P., & Monatanarella, L. (2016). Mapping topsoil physical properties at European scale using the LUCAS database. *Geoderma*, *261*, 110–123. https://doi.org/10.1016/j.geoderma.2015.07.006

Blyth, E. M., Arora, V. K., Clark, D. B., Dadson, S. J., De Kauwe, M. G., Lawrence, D. M., et al. (2021). Advances in land surface modelling. *Current Climate Change Reports*, *7*(2), 45–71. https://doi.org/10.1007/s40641-021-00171-5

Boas, T., Bogena, H., Grünwald, T., Heinesch, B., Ryu, D., Schmidt, M., et al. (2021). Improving the representation of cropland sites in the Community Land Model (CLM) version 5.0. *Geoscientific Model Development*, *14*(1), 573–601. https://doi.org/10.5194/gmd-14-573-2021

Bogena, H., Herbst, M., Huisman, J. A., Rosenbaum, U., Weuthen, A., & Vereecken, H. (2010). Potential of wireless sensor networks for measuring soil water content variability. *Vadose Zone Journal*, *9*(4), 1002–1013. https://doi.org/10.2136/vzj2009.0173

Bogena, H., Weuthen, A., & Huisman, J. A. (2022). Recent developments in wireless soil moisture sensing to support scientific research and agricultural management. *Sensors*, *22*(24), 9792. https://doi.org/10.3390/s22249792

Bogena, H., White, T., Bour, O., Li, X., & Jensen, K. H. (2018). Toward better understanding of terrestrial processes through long-term hydrological observatories. *Vadose Zone Journal*, *17*(1), 1–10. https://doi.org/10.2136/vzj2018.10.0194

Brogi, C., Pisinaras, V., Köhli, M., Dombrowski, O., Hendricks Franssen, H.-J., Babakos, K., et al. (2023). Monitoring irrigation in small orchards with cosmic-ray neutron sensors. *Sensors*, *23*(5), 2378. https://doi.org/10.3390/s23052378

Budak, H., Kantar, M., & Yucebilgili Kurtoglu, K. (2013). Drought tolerance in modern and wild wheat. *The Scientific World Journal*, *2013*, 1–16. https://doi.org/10.1155/2013/548246

Burgess, S. S. O. (2018). *SFM1 sap flow meter manual, version 5.1*. ICT International Pty Ltd.

Cai, X., McKinney, D. C., & Rosegrant, M. W. (2003). Sustainability analysis for irrigation water management in the Aral Sea region. *Agricultural Systems*, *76*(3), 1043–1066. https://doi.org/10.1016/S0308-521X(02)00028-8

Caswell, T. A., Droettboom, M., Lee, A., Hunter, J., Firing, E., Sales De Andrade, E., et al. (2022). matplotlib/matplotlib: Rel: v3.5.2 [Software]. https://doi.org/10.5281/zenodo.6513224

Chaves, M. M., Maroco, J. P., & Pereira, J. S. (2003). Understanding plant responses to drought—From genes to the whole plant. *Functional Plant Biology*, *30*(3), 239–264. https://doi.org/10.1071/FP02076

Cheng, Y., Huang, M., Chen, M., Guan, K., Bernacchi, C., Peng, B., & Tan, Z. (2020). Parameterizing perennial bioenergy crops in Version 5 of the Community Land Model based on site-level observations in the Central Midwestern United States. *Journal of Advances in Modeling Earth Systems*, *12*(1), 1–24. https://doi.org/10.1029/2019MS001719

Clapp, R. B., & Hornberger, G. M. (1978). Empirical equations for some soil hydraulic properties. *Water Resources Research*, *14*(4), 601–604. https://doi.org/10.1029/WR014i004p00601

Copernicus. (2016). European digital elevation model (EU- DEM), version 1.1. Retreived 13/09/2022 from Retrieved from https://land.copernicus.eu/imagery-in-situ/eu-dem/eu-dem-v1.1?tab=metadata

Cosby, B. J., Hornberger, G. M., Clapp, R. B., & Ginn, T. R. (1984). A statistical exploration of the relationships of soil moisture characteristics to the physical properties of soils. *Water Resources Research*, *20*(6), 682–690. https://doi.org/10.1029/WR020i006p00682

Dangar, S., Asoka, A., & Mishra, V. (2021). Causes and implications of groundwater depletion in India: A review. *Journal of Hydrology*, *596*, 126103. https://doi.org/10.1016/j.jhydrol.2021.126103

Dawson, N., Fischer, J., Kuhn, M., Pasotti, A., Mhugent, Sutton, T., et al. (2022). qgis/QGIS: 3.22.4 [Software]. https://doi.org/10.5281/zenodo.6139225

DeAngelis, A., Dominguez, F., Fan, Y., Robock, A., Kustu, M. D., & Robinson, D. (2010). Evidence of enhanced precipitation due to irrigation over the Great Plains of the United States. *Journal of Geophysical Research*, *115*(D15). https://doi.org/10.1029/2010JD013892

Dercas, N., Dalezios, N. R., Stamatiadis, S., Evangelou, E., Glampedakis, A., Mantonanakis, G., & Tserlikakis, N. (2022). AquaCrop simulation of winter wheat under different N management practices. *Hydrology*, *9*(4), 56. https://doi.org/10.3390/hydrology9040056

de Vrese, P., Hagemann, S., & Claussen, M. (2016). Asian irrigation, African rain: Remote impacts of irrigation. *Geophysical Research Letters*, *43*(8), 3737–3745. https://doi.org/10.1002/2016GL068146

Dingman, S. L. (2015). *Physical hydrology*. Waveland press.

Dombrowski, O. (2022). odombro/CTSM: CLM5-FruitTree: A new sub-model for deciduous fruit trees [Software]. https://doi.org/10.5281/zenodo.8154390

Dombrowski, O., & Bogena, H. R. (2023). Soil moisture, soil matric potential, meteorological variables, sap flow, and irrigation measurements during an irrigation study in two apple orchards in Pinios Hydrologic Observatory, Greece, from 2020 to 2022 [Dataset]. https://doi.org/10.34731/e1ss-pc69

Dombrowski, O., Brogi, C., Hendricks Franssen, H.-J., Zanotelli, D., & Bogena, H. (2022). CLM5-FruitTree: A new sub-model for deciduous fruit trees in the community land model (CLM5). *Geoscientific Model Development*, *15*(13), 5167–5193. https://doi.org/10.5194/gmd-15-5167-2022

Dombrowski, O., Hendricks Franssen, H. J., Brogi, C., & Bogena, H. R. (2021). Performance of the ATMOS41 all-in-one weather station for weather monitoring. *Sensors*, *21*(3), 741. https://doi.org/10.3390/s21030741

Elliott, J., Deryng, D., Müller, C., Frieler, K., Konzmann, M., Gerten, D., et al. (2014). Constraints and potentials of future irrigation water availability on agricultural production under climate change. *Proceedings of the National Academy of Sciences*, *111*(9), 3239–3244. https://doi.org/10.1073/pnas.1222474110

Erb, K. H., Luyssaert, S., Meyfroidt, P., Pongratz, J., Don, A., Kloster, S., et al. (2017). Land management: Data availability and process understanding for global change studies. *Global Change Biology*, *23*(2), 512–533. https://doi.org/10.1111/gcb.13443

Eshete, D. G., Sinshaw, B. G., & Legese, K. G. (2020). Critical review on improving irrigation water use efficiency: Advances, challenges, and opportunities in the Ethiopia context. *Water-Energy Nexus*, *3*, 143–154. https://doi.org/10.1016/j.wen.2020.09.001

Fader, M., von Bloh, W., Shi, S., Bondeau, A., & Cramer, W. (2015). Modelling Mediterranean agro-ecosystems by including agricultural trees in the LPJmL model. *Geoscientific Model Development*, *8*(11), 3545–3561. https://doi.org/10.5194/gmd-8-3545-2015

Fan, Y., Roupsard, O., Bernoux, M., Le Maire, G., Panferov, O., Kotowska, M. M., & Knohl, A. (2015). A sub-canopy structure for simulating oil palm in the community land model (CLM-Palm): Phenology, allocation and yield. *Geoscientific Model Development*, *8*(11), 3785–3800. https://doi.org/10.5194/gmd-8-3785-2015

FAO. (2023). Crop information - potato. Retrieved 19/06/2023 from Retrieved from https://www.fao.org/land-water/databases-and-software/crop-information/potato/en/

Felfelani, F., Pokhrel, Y., Guan, K., & Lawrence, D. M. (2018). Utilizing SMAP soil moisture data to constrain irrigation in the Community Land Model. *Geophysical Research Letters*, *45*(23), 12892–12902. https://doi.org/10.1029/2018GL080870

Ferguson, I. M., & Maxwell, R. M. (2012). Human impacts on terrestrial hydrology: Climate change versus pumping and irrigation. *Environmental Research Letters*, *7*(4), 044022. https://doi.org/10.1088/1748-9326/7/4/044022

Gao, X., Avramov, A., Saikawa, E., & Schlosser, C. A. (2021). Emulation of Community Land Model version 5 (CLM5) to quantify sensitivity of soil moisture to uncertain parameters. *Journal of Hydrometeorology*, *22*(2), 259–278. https://doi.org/10.1175/JHM-D-20-0043.1

García-Garizábal, I., Causapé, J., & Abrahão, R. (2012). Nitrate contamination and its relationship with flood irrigation management. *Journal of Hydrology*, *442*, 15–22. https://doi.org/10.1016/j.jhydrol.2012.03.017

Gilley, J. R., & Watts, D. G. (1977). Energy reduction through improved irrigation practices. In *Agriculture and energy* (pp. 187–203). Elsevier. https://doi.org/10.1016/B978-0-12-454250-1.50019-8

Gordon, L. J., Steffen, W., Jönsson, B. F., Folke, C., Falkenmark, M., & Johannessen, Å. (2005). Human modification of global water vapor flows from the land surface. *Proceedings of the National Academy of Sciences*, *102*(21), 7612–7617. https://doi.org/10.1073/pnas.0500208102

Gurung, T. R., Bousquet, F., & Trébuil, G. (2006). Companion modeling, conflict resolution, and institution building: Sharing irrigation water in the lingmuteychu watershed, Bhutan. *Ecology and Society*, *11*(2), art36. https://doi.org/10.5751/es-01929-110236

Han, X., Franssen, H.-J. H., Rosolem, R., Jin, R., Li, X., & Vereecken, H. (2015). Correction of systematic model forcing bias of CLM using assimilation of cosmic-ray neutrons and land surface temperature: A study in the heihe catchment, China. *Hydrology and Earth System Sciences*, *19*(1), 615–629. https://doi.org/10.5194/hess-19-615-2015

Hiederer, R. (2013). Mapping soil properties for Europe—Spatial representation of soil database attributes, *47*, 1831–9424, https://doi.org/10.2788/94128

Huang, Y., Zhang, Z., Li, Z., Dai, D., & Li, Y. (2022). Evaluation of water use efficiency and optimal irrigation quantity of spring maize in Hetao Irrigation District using the Noah-MP Land Surface Model. *Agricultural Water Management*, *264*, 107498. https://doi.org/10.1016/j.agwat.2022.107498

Ibragimov, N., Evett, S. R., Esanbekov, Y., Kamilov, B. S., Mirzaev, L., & Lamers, J. P. (2007). Water use efficiency of irrigated cotton in Uzbekistan under drip and furrow irrigation. *Agricultural Water Management*, *90*(1–2), 112–120. https://doi.org/10.1016/j.agwat.2007.01.016

Kennedy, D., Swenson, S., Oleson, K. W., Lawrence, D. M., Fisher, R., Lola da Costa, A. C., & Gentine, P. (2019). Implementing plant hydraulics in the community land model, version 5. *Journal of Advances in Modeling Earth Systems*, *11*(2), 485–513. https://doi.org/10.1029/2018MS001500

Lange, S., & Büchner, M. (2020). ISIMIP2a atmospheric climate input data (v1.0). https://doi.org/10.48364/ISIMIP.886955

Latinopoulos, P. (2005). Valuation and pricing of irrigation water: An analysis in Greek agricultural areas. *Global NEST Journal*, *7*(3), 323–335. https://www.academia.edu/download/78294925/5e06df21cbbf097a1b9ee71b541840583c94.pdf

Lawrence, D., Fisher, R., Koven, C., Oleson, K., Swenson, S., Vertenstein, M., et al. (2018). Technical description of version 5.0 of the community land model (CLM). *Natl. Cent. Atmospheric Res. (NCAR)*. Retrieved from http://www.cesm.ucar.edu/models/cesm2/land/CLM50_Tech_Note.pdf. (last access 2 May 2021.

Lawrence, D., & Slater, A. (2008). Incorporating organic soil into a global climate model. *Climate Dynamics*, *30*(2–3), 145–160. https://doi.org/10.1007/s00382-007-0278-1

Lawrence, D. M., Fisher, R. A., Koven, C. D., Oleson, K. W., Swenson, S. C., Bonan, G., et al. (2019). The community land model version 5: Description of new features, benchmarking, and impact of forcing uncertainty. *Journal of Advances in Modeling Earth Systems*, *11*(12), 4245–4287. https://doi.org/10.1029/2018MS001583

Lawston, P. M., Santanello, J. A., Jr., Franz, T. E., & Rodell, M. (2017). Assessment of irrigation physics in a land surface modeling framework using non-traditional and human-practice datasets. *Hydrology and Earth System Sciences*, *21*(6), 2953–2966. https://doi.org/10.5194/hess-21-2953-2017

Leng, G., Huang, M., Tang, Q., Gao, H., & Leung, L. R. (2014). Modeling the effects of groundwater-fed irrigation on terrestrial hydrology over the conterminous United States. *Journal of Hydrometeorology*, *15*(3), 957–972. https://doi.org/10.1175/JHM-D-13-049.1

Leng, G., Huang, M., Tang, Q., & Leung, L. R. (2015). A modeling study of irrigation effects on global surface water and groundwater resources under a changing climate. *Journal of Advances in Modeling Earth Systems*, *7*(3), 1285–1304. https://doi.org/10.1002/2015MS000437

Leng, G., Huang, M., Tang, Q., Sacks, W. J., Lei, H., & Leung, L. R. (2013). Modeling the effects of irrigation on land surface fluxes and states over the conterminous United States: Sensitivity to input data and model parameters. *Journal of Geophysical Research: Atmospheres*, *118*(17), 9789–9803. https://doi.org/10.1002/jgrd.50792

Leng, G., Leung, L. R., & Huang, M. (2017). Significant impacts of irrigation water sources and methods on modeling irrigation effects in the ACME Land Model. *Journal of Advances in Modeling Earth Systems*, *9*(3), 1665–1683. https://doi.org/10.1002/2016MS000885

Levis, S., Bonan, G. B., Kluzek, E., Thornton, P. E., Jones, A., Sacks, W. J., & Kucharik, C. J. (2012). Interactive crop management in the Community Earth System Model (CESM1): Seasonal influences on land–atmosphere fluxes. *Journal of Climate*, *25*(14), 4839–4859. https://doi.org/10.1175/JCLI-D-11-00446.1

Li, D., Franssen, H.-J. H., Han, X., Jiménez-Bello, M. A., Alzamora, F. M., & Vereecken, H. (2018). Evaluation of an operational real-time irrigation scheduling scheme for drip irrigated citrus fields in Picassent, Spain. *Agricultural Water Management*, *208*, 465–477. https://doi.org/10.1016/j.agwat.2018.06.022

Liu, X., Chen, F., Barlage, M., Zhou, G., & Niyogi, D. (2016). Noah-MP-Crop: Introducing dynamic crop growth in the Noah-MP land surface model. *Journal of Geophysical Research: Atmospheres*, *121*(23), 13953–13972. https://doi.org/10.1002/2016JD025597

Lombardozzi, D. L., Lu, Y., Lawrence, P. J., Lawrence, D. M., Swenson, S., Oleson, K. W., et al. (2020). Simulating agriculture in the community land model version 5. *Journal of Geophysical Research: Biogeosciences*, *125*(8), 1–19. https://doi.org/10.1029/2019JG005529

Mattas, K., Tsakiridou, E., Karelakis, C., Kallirroi, N., Gatsikos, A., & Papadopoulos, I. (2019). PDO zagora and PGI kastoria apples in Greece. *Sustainability of European Food Quality Schemes: Multi-Performance, Structure, and Governance of PDO, PGI, and Organic Agri-Food Systems*, 231–264. https://doi.org/10.1007/978-3-030-27508-2_13

McDermid, S., Nocco, M., Lawston-Parker, P., Keune, J., Yadu Pokhrel, M. J., Jägermeyr, J., et al. (2023). Irrigation in the Earth system. *Nature Reviews Earth and Environment*, *4*(7), 435–453. https://doi.org/10.1038/s43017-023-00438-5

McLaughlin, D., & Kinzelbach, W. (2015). Food security and sustainable resource management. *Water Resources Research*, *51*(7), 4966–4985. https://doi.org/10.1002/2015WR017053

Mueller, N. D., Gerber, J. S., Johnston, M., Ray, D. K., Ramankutty, N., & Foley, J. A. (2012). Closing yield gaps through nutrient and water management. *Nature*, *490*(7419), 254–257. https://doi.org/10.1038/nature11420

Nasri, B., Fouché, O., & Torri, D. (2015). Coupling published pedotransfer functions for the estimation of bulk density and saturated hydraulic conductivity in stony soils. *Catena*, *131*, 99–108. https://doi.org/10.1016/j.catena.2015.03.018

Nijland, W., Van der Meijde, M., Addink, E. A., & De Jong, S. M. (2010). Detection of soil moisture and vegetation water abstraction in a Mediterranean natural area using electrical resistivity tomography. *Catena*, *81*(3), 209–216. https://doi.org/10.1016/j.catena.2010.03.005

Ozdogan, M., & Gutman, G. (2008). A new methodology to map irrigated areas using multi-temporal MODIS and ancillary data: An application example in the continental US. *Remote Sensing of Environment*, *112*(9), 3520–3537. https://doi.org/10.1016/j.rse.2008.04.010

Ozdogan, M., Rodell, M., Beaudoing, H. K., & Toll, D. L. (2010). Simulating the effects of irrigation over the United States in a land surface model based on satellite-derived agricultural data. *Journal of Hydrometeorology*, *11*(1), 171–184. https://doi.org/10.1175/2009JHM1116.1

Panagopoulos, A., Herrmann, F., Pisinaras, V., & Wendland, F. (2018). Impact of climate change on irrigation need and groundwater resources in pinios basin. *paper presented at Proceedings, MDPI AG*.

Panagoulia, D. (1995). Assessment of daily catchment precipitation in mountainous regions for climate change interpretation. *Hydrological Sciences Journal*, *40*(3), 331–350. https://doi.org/10.1080/02626669509491419

Peng, B., Guan, K., Chen, M., Lawrence, D. M., Pokhrel, Y., Suyker, A., et al. (2018). Improving maize growth processes in the community land model: Implementation and evaluation. *Agricultural and Forest Meteorology*, *250*, 64–89. https://doi.org/10.1016/j.agrformet.2017.11.012

Peng, B., Guan, K., Tang, J., Ainsworth, E. A., Asseng, S., Bernacchi, C. J., et al. (2020). Towards a multiscale crop modelling framework for climate change adaptation assessment. *Nature Plants*, *6*(4), 338–348. https://doi.org/10.1038/s41477-020-0625-3

Pisinaras, V., Herrmann, F., Panagopoulos, A., Tziritis, E., McNamara, I., & Wendland, F. (2023). Fully distributed water balance modelling in large agricultural areas—The pinios river basin (Greece) case study. *Sustainability*, *15*(5), 4343. https://doi.org/10.3390/su15054343

Pisinaras, V., Panagopoulos, A., Herrmann, F., Bogena, H. R., Doulgeris, C., Ilias, A., et al. (2018). Hydrologic and geochemical research at pinios hydrologic observatory: Initial results. *Vadose Zone Journal*, *17*(1), 1–16. https://doi.org/10.2136/vzj2018.05.0102

Poesen, J., & Lavee, H. (1994). Rock fragments in top soils: Significance and processes. *Catena*, *23*(1–2), 1–28. https://doi.org/10.1016/0341-8162(94)90050-7

Pokhrel, Y. N., Hanasaki, N., Wada, Y., & Kim, H. (2016). Recent progresses in incorporating human land–water management into global land surface models toward their integration into Earth system models. *Wiley Interdisciplinary Reviews: Water*, *3*(4), 548–574. https://doi.org/10.1002/wat2.1150

Pongratz, J., Dolman, H., Don, A., Erb, K. H., Fuchs, R., Herold, M., et al. (2018). Models meet data: Challenges and opportunities in implementing land management in Earth system models. *Global Change Biology*, *24*(4), 1470–1487. https://doi.org/10.1111/gcb.13988

PythonSoftwareFoundation. (2023). Python language reference, version 3.10.4 [Software]. Retrieved from https://www.python.org/downloads/release/python-3104/

Sacks, W. J., Cook, B. I., Buenning, N., Levis, S., & Helkowski, J. H. (2009). Effects of global irrigation on the near-surface climate. *Climate Dynamics*, *33*(2–3), 159–175. https://doi.org/10.1007/s00382-008-0445-z

Scanlon, B. R., Faunt, C. C., Longuevergne, L., Reedy, R. C., Alley, W. M., McGuire, V. L., & McMahon, P. B. (2012). Groundwater depletion and sustainability of irrigation in the US high plains and central valley. *Proceedings of the National Academy of Sciences*, *109*(24), 9320–9325. https://doi.org/10.1073/pnas.1200311109

Sherman, W., & Beckman, T. (2002). Climatic adaptation in fruit crops. In *Paper Presented at XXVI International Horticultural Congress: Genetics and Breeding of Tree Fruits and Nuts* (Vol. *622*).

Shrestha, P., Kurtz, W., Vogel, G., Schulz, J. P., Sulis, M., Hendricks Franssen, H. J., et al. (2018). Connection between root zone soil moisture and surface energy flux partitioning using modeling, observations, and data assimilation for a temperate grassland site in Germany. *Journal of Geophysical Research: Biogeosciences*, *123*(9), 2839–2862. https://doi.org/10.1029/2016JG003753

Siebert, S., Döll, P., Hoogeveen, J., Faures, J. M., Frenken, K., & Feick, S. (2005). Development and validation of the global map of irrigation areas. *Hydrology and Earth System Sciences*, *9*(5), 535–547. https://doi.org/10.5194/hess-9-535-2005

Smith, P., De Noblet-Ducoudré, N., Ciais, P., Peylin, P., Viovy, N., Meurdesoif, Y., & Bondeau, A. (2010). European-wide simulations of croplands using an improved terrestrial biosphere model: Phenology and productivity. *Journal of Geophysical Research*, *115*(G1). https://doi.org/10.1029/2008JG000800

Strebel, L., Bogena, H. R., Vereecken, H., & Hendricks Franssen, H.-J. (2022). Coupling the community land model version 5.0 to the parallel data assimilation framework PDAF: Description and applications. *Geoscientific Model Development*, *15*(2), 395–411. https://doi.org/10.5194/gmd-15-395-2022

Swenson, S. (2023). swensosc/ctsm: Mct irrigation stream [Software]. https://doi.org/10.5281/zenodo.8290143

TERENO. (2023a). TERrestrial ENvironment Observatories data portal [Dataset]. Retrieved from https://hdl.handle.net/20.500.11952/TERENO/00000708. *AGIA_K_001*

TERENO. (2023b). TERrestrial ENvironment Observatories data portal [Dataset]. Retrieved from https://hdl.handle.net/20.500.11952/TERENO/00000709. *AGIA_K_002*

TERENO. (2023c). TERrestrial ENvironment Observatories data portal [Dataset]. Retrieved from https://hdl.handle.net/20.500.11952/TERENO/1056009574. *AGIA_CK_003*

Tsakmakis, I., Babakos, K., Chatzi, A., Pisinaras, V., Brogi, C., Bogena, H., et al. (2023). *Precision irrigation scheduling through high frequency data monitoring. Implementation in apple orchard cultivations - central Greece*. EGU General Assembly 2023. 24–28 Apr 2023, EGU23. https://doi.org/10.5194/egusphere-egu23-5186.5186

Viovy, N. (2018). CRUNCEP version 7 - atmospheric forcing data for the community land model [Dataset]. https://doi.org/10.5065/PZ8F-F017. *Research Data Archive at the National Center for Atmospheric Research, Computational and Information Systems Laboratory*

Wada, Y., Van Beek, L. P., Van Kempen, C. M., Reckman, J. W., Vasak, S., & Bierkens, M. F. (2010). Global depletion of groundwater resources. *Geophysical Research Letters*, *37*(20). https://doi.org/10.1029/2010GL044571

Wentworth, C. K. (1922). A scale of grade and class terms for clastic sediments. *The Journal of Geology*, *30*(5), 377–392. https://doi.org/10.1086/622910

Xia, Q., Liu, P., Fan, Y., Cheng, L., An, R., Xie, K., & Zhou, L. (2022). Representing irrigation processes in the land surface-hydrological model and a case study in the yangtze river basin, China. *Journal of Advances in Modeling Earth Systems*, *14*(7), e2021MS002653. https://doi.org/10.1029/2021MS002653

Yao, Y., Vanderkelen, I., Lombardozzi, D., Swenson, S., Lawrence, D., Jägermeyr, J., et al. (2022). Implementation and evaluation of irrigation techniques in the community land model. *Journal of Advances in Modeling Earth Systems*, *14*(12). https://doi.org/10.1029/2022MS003074

Yin, Z., Wang, X., Ottlé, C., Zhou, F., Guimberteau, M., Polcher, J., et al. (2020). Improvement of the irrigation scheme in the ORCHIDEE land surface model and impacts of irrigation on regional water budgets over China. *Journal of Advances in Modeling Earth Systems*, *12*(4), e2019MS001770. https://doi.org/10.1029/2019MS001770

Zacharias, S., Loescher, H. W., Bogena, H., Kiese, R., Schrön, M., Attinger, S., et al. (2024). 15 years of integrated terrestrial environmental observatories (TERENO) in Germany: Functions, services and lessons learned. *Authorea Preprints*. https://doi.org/10.22541/essoar.170808463.36288013/v1

Zalidis, G., Stamatiadis, S., Takavakoglou, V., Eskridge, K., & Misopolinos, N. (2002). Impacts of agricultural practices on soil and water quality in the Mediterranean region and proposed assessment methodology. *Agriculture, Ecosystems and Environment*, *88*(2), 137–146. https://doi.org/10.1016/S0167-8809(01)00249-3

Zhang, Y., Hou, K., Qian, H., Gao, Y., Fang, Y., Xiao, S., et al. (2022). Characterization of soil salinization and its driving factors in a typical irrigation area of Northwest China. *Science of the Total Environment*, *837*, 155808. https://doi.org/10.1016/j.scitotenv.2022.155808

Zhang, Z., Barlage, M., Chen, F., Li, Y., Helgason, W., Xu, X., et al. (2020). Joint modeling of crop and irrigation in the central United States using the Noah-MP land surface model. *Journal of Advances in Modeling Earth Systems*, *12*(7), e2020MS002159. https://doi.org/10.1029/2020MS002159

Zhu, B., Huang, M., Cheng, Y., Xie, X., Liu, Y., Zhang, X., et al. (2020). Effects of irrigation on water, carbon, and nitrogen budgets in a semiarid watershed in the pacific northwest: A modeling study. *Journal of Advances in Modeling Earth Systems*, *12*(9), e2019MS001953. https://doi.org/10.1029/2019MS001953